



AN ABSTRACT OF THE THESIS OF

Victor Q. Dang for the degree of Honors Bachelor of Science in Mechanical Engineering presented on June 04, 2013. Title: The Design, Manufacturing, and Testing of an Undertray for Formula SAE.

Abstract Approved:

---

Robert Paasch

A student-built lap time simulation coupled with the scoring model of the Formula Society of Automotive Engineers (SAE) Series has revealed the major importance of downforce on overall points. As a result, the Global Formula Racing (GFR) team has recently focused much effort towards the development of an aerodynamics package for their Formula SAE racecars. One component of the aerodynamics package is the undertray, a device that exploits the underbody airflow to generate downforce. This thesis details the development of the undertray used for the 2013 GFR aerodynamics package, including the aerodynamic design, mechanical design, manufacturing, and physical validation. The 2013 undertray is a simple inverted airfoil concept inspired by the Lotus Type 78 F-1 car.

Key Words: Aerodynamics Formula SAE Undertray

Corresponding E-mail Address: victorqdang@gmail.com

© Copyright by Victor Q. Dang

June 04, 2013

All Rights Reserved

The Design, Manufacturing, and Testing of an Undertray for Formula SAE

by

Victor Q. Dang

A PROJECT

submitted to

Oregon State University

University Honors College

in partial fulfillment of the requirements for the degree of

Honors Bachelors of Science in Mechanical Engineering (Honors Associate)

Presented June 04, 2013

Commencement June 15, 2013

Honors Bachelor of Science in Mechanical Engineering project of Victor Q. Dang  
presented on June 04, 2013.

APPROVED:

---

Mentor, representing Mechanical Engineering

---

Committee Member, representing Mechanical Engineering

---

Committee Member, representing Mechanical Engineering

---

Department Head, Mechanical, Industrial, and Manufacturing Engineering (MIME)

---

Dean, University Honors College

I understand that my project will become part of the permanent collection of Oregon State University, University Honors College. My signature below authorizes release of my project to any reader upon request.

---

Victor Q. Dang, Author

## **ACKNOWLEDGEMENTS**

I would like to thank all of my teammates on the Global Formula Racing Team for making this thesis possible. In particular, I would like to thank Dr. Robert Paasch, Trevor Takaro, Jill Lewis, Robert Story, Manuel Sturm, Phillip Arscott, Brittany Burns, Ben Cox, Sven Dugojevic, Chris Jenista, Clayton Wilson, Matthew Drager, Tim Bender, and Edgar Iliev for their contribution to this project specifically.

## TABLE OF CONTENTS

<b>1. INTRODUCTION .....</b>	<b>15</b>
<b>2. BACKGROUND .....</b>	<b>17</b>
<b>2.1. Aerodynamics .....</b>	<b>17</b>
2.1.1. Underbody Aerodynamics .....	17
2.1.2. Computational Fluid Dynamics .....	18
2.1.3. Physical Testing .....	18
<b>2.2. Carbon Fiber Manufacturing .....</b>	<b>18</b>
2.2.1. Pre-Impregnated Carbon Fiber .....	19
2.2.2. Sandwich Structures.....	19
2.2.3. Composite Design.....	19
<b>3. CONCEPTUAL DESIGN .....</b>	<b>21</b>
<b>3.1. Requirements.....</b>	<b>21</b>
3.1.1. General Quantitative Requirements.....	21
3.1.2. Formula SAE Competition Requirements .....	22
3.1.3. Equating design parameters to points .....	23
3.1.4. General Qualitative Requirements .....	23
3.1.5. Formula SAE Rules and Requirements .....	25

## Table of Contents (continued)

3.2. Initial Concept .....	25
<b>4. AERODYNAMIC DESIGN.....</b>	<b>29</b>
4.1. Aerodynamic Behavior .....	29
4.2. Undertray Additions .....	30
4.3. Splitter Study .....	31
4.4. Endplate Study .....	33
4.5. Aerodynamic Design Summary .....	34
<b>5. MECHANICAL DESIGN .....</b>	<b>35</b>
5.1. Materials Available .....	35
5.2. Undertray Airfoil Section Structure.....	36
5.2.1. Wing Halves.....	37
5.2.1.1. <i>Wing Halves Layup Schedule</i> .....	37
5.2.1.2. <i>Wing Halves Bonding Areas</i> .....	38
5.2.2. Gurney Flap .....	41
5.2.2.1. <i>Gurney Flap Layup Schedule</i> .....	41
5.2.3. Spar .....	42
5.2.3.1. <i>Spar Layup Schedule</i> .....	43
5.2.4. Endplate .....	43

## Table of Contents (Continued)

5.2.4.1. <i>Endplate Layup Schedule</i> .....	44
5.2.5. Wing Inserts .....	45
5.2.5.1. <i>Wing Insert Layup Schedule</i> .....	45
<b>5.3. Undertray Integration.....</b>	<b>47</b>
5.3.1. Flanges .....	48
5.3.1.1. <i>Flange Bonding Area</i> .....	49
5.3.1.2. <i>Flange Bolt hole locations</i> .....	50
5.3.1.3. <i>Test Sample</i> .....	51
5.3.1.4. <i>c-Car Flange Layup Schedule</i> .....	53
5.3.1.5. <i>e-Car Flange Layup Schedule</i> .....	54
5.3.2. Drop Link.....	55
<b>5.4. Splitter Structure and Integration.....</b>	<b>55</b>
5.4.1. Splitter Flat Plate.....	56
5.4.1.1. <i>Splitter Flat Plate Layup Schedule</i> .....	56
5.4.2. Splitter Panels Layup Schedule .....	57
5.4.2.1. <i>Splitter Panels Layup Schedule</i> .....	57
5.4.3. Brackets.....	57
<b>5.5. Mechanical Design Summary.....</b>	<b>58</b>
<b>6. MANUFACTURING DESIGN .....</b>	<b>60</b>

## Table of Contents (Continued)

<b>6.1. Materials Available .....</b>	<b>60</b>
<b>6.2. Undertray Mold (Airfoil Section) .....</b>	<b>60</b>
<b>6.3. Undertray Wing Insert Mold .....</b>	<b>63</b>
<b>6.4. Undertray Endplate Mold .....</b>	<b>64</b>
<b>6.5. Undertray Top Flange Mold .....</b>	<b>66</b>
<b>6.6. Undertray Bottom Flange Mold.....</b>	<b>67</b>
<b>6.7. Remaining Molds and Tools.....</b>	<b>68</b>
<b>6.8. Manufacturing Design Summary .....</b>	<b>68</b>
<b>7. MANUFACTURING .....</b>	<b>71</b>
<b>7.1. Tooling Parts.....</b>	<b>71</b>
7.1.1. Undertray Airfoil Section Molds .....	71
7.1.1.1. <i>Making the Stock for the Undertray Airfoil Section Molds</i> .....	71
7.1.1.2. <i>CNC Machining the Undertray Airfoil Section Molds</i> .....	73
7.1.1.3. <i>Finishing the Undertray Airfoil Section Molds</i> .....	75
7.1.2. Undertray Wing Insert Mold.....	75
7.1.2.1. <i>Making the Stock for the Wing Insert Mold</i> .....	75
7.1.2.2. <i>CNC Machining the Wing Insert Mold</i> .....	76
7.1.2.3. <i>Finishing the Wing Insert Mold</i> .....	78
7.1.3. Undertray Endplate Mold .....	79

## Table of Contents (Continued)

7.1.3.1. <i>Making the Stock for the Undertray Endplate Mold</i> .....	79
7.1.3.2. <i>CNC Machining the Undertray Endplate Mold</i> .....	80
7.1.3.3. <i>Finishing the Undertray Endplate Mold</i> .....	81
7.1.4. Undertray Flange Molds .....	82
7.1.4.1. <i>Making the Stock for the Undertray Flange Molds</i> .....	82
7.1.4.2. <i>CNC Machining the Undertray Flange Molds</i> .....	82
7.1.4.3. <i>Finishing the Undertray Flange Molds</i> .....	83
<b>7.2. Carbon Fiber Parts</b> .....	<b>84</b>
7.2.1. Oven Cures.....	85
7.2.2. Undertray Airfoil Sections.....	85
7.2.2.1. <i>Templates for Undertray Airfoil Section</i> .....	85
7.2.2.2. <i>Layup of the Undertray Airfoil Sections</i> .....	86
7.2.3. Undertray Wing Inserts.....	88
7.2.3.1. <i>Templates for the Undertray Wing Insert</i> .....	88
7.2.3.2. <i>Layup of the Undertray Wing Inserts</i> .....	89
7.2.4. Undertray Endplate .....	90
7.2.4.1. <i>Making the Hard-points for the Undertray Endplate</i> .....	90
7.2.4.2. <i>Layup of the Undertray Endplate</i> .....	91
7.2.5. Undertray Flanges.....	93

## Table of Contents (Continued)

7.2.6.    Spars and Gurney Flaps .....	94
7.2.7.    Undertray Splitter.....	94
7.2.7.1. <i>Template for the Splitter Flat Plate</i> .....	94
7.2.7.2. <i>Layup of the Splitter Flat Plate</i> .....	95
7.2.7.1. <i>Layup of the Splitter Panels</i> .....	96
<b>    7.3.    Finishing.....</b>	<b>97</b>
7.3.1.    Trimming .....	97
7.3.2.    Bonding.....	99
7.3.2.1. <i>Weld Nuts to Wing Insert</i> .....	99
7.3.2.2. <i>Undertray Airfoil, Spar, and Wing Insert</i> .....	100
<b>    7.4.    Undertray Airfoil Section Integration.....</b>	<b>101</b>
7.4.1.    Locating on the Chassis .....	101
7.4.2.    Mounting the Undertray Airfoil Section to the Chassis.....	103
7.4.3.    Finishing Touches .....	104
<b>    7.5.    Undertray Splitter Section Integration .....</b>	<b>105</b>
7.5.1.    Splitter Flat Plate Integration .....	105
7.5.1.    Splitter Panel Integration .....	106
7.5.1.    Mounting the Splitter to the Chassis .....	106
<b>    7.6.    Manufacturing Summary .....</b>	<b>107</b>

## Table of Contents (Continued)

<b>8. TESTING .....</b>	<b>108</b>
<b>    8.1. Aerodynamic Testing.....</b>	<b>108</b>
8.1.1. On-Off Testing.....	108
8.1.2. Coast-Down Testing .....	108
8.1.3. Pressure Tapping.....	109
8.1.3.1. <i>Raw Data</i> .....	110
8.1.3.2. <i>Pressure Gradient Results</i> .....	111
8.1.1. Aerodynamic Testing Summary .....	114
<b>    8.2. Mechanical Testing .....</b>	<b>114</b>
8.2.1. Actual Mass .....	114
8.2.2. Mechanical Failures .....	115
<b>9. CONCLUSION.....</b>	<b>118</b>
<b>10. WORKS CITED .....</b>	<b>119</b>

## LIST OF FIGURES

<i>Figure 1: GFR 2013 undertray baseline concept .....</i>	26
<i>Figure 2: GFR 2013 undertray baseline velocity vectors .....</i>	29
<i>Figure 3: GFR 2013 undertray baseline pressure gradient .....</i>	30
<i>Figure 4: GFR 2013 undertray concept .....</i>	31
<i>Figure 5: Curvy splitter .....</i>	31
<i>Figure 6: New rectangular splitter.....</i>	32
<i>Figure 7: Undertray with the new endplate concept .....</i>	33
<i>Figure 8: Final undertray aerodynamic design.....</i>	34
<i>Figure 9: Undertray Airfoil Section exploded view.....</i>	36
<i>Figure 10: Side-View of the layup schedule used for undertray airfoil sections.....</i>	37
<i>Figure 11: Front-view cross section of the undertray airfoil sections .....</i>	38
<i>Figure 12: Trailing edge bonding area .....</i>	39
<i>Figure 13: Two wing halves joined together by a butt joint .....</i>	39
<i>Figure 14: Joggle concept for bonding the two wing halves together .....</i>	40
<i>Figure 15: Layup schedule used for gurney flaps .....</i>	41
<i>Figure 16: Undertray spar.....</i>	42
<i>Figure 17: Layup schedule used for spars.....</i>	43
<i>Figure 18: Layup schedule used for undertray endplates .....</i>	44
<i>Figure 19: Layup schedule used for undertray endplate skirts .....</i>	44
<i>Figure 20: Layup schedule used for the wing inserts .....</i>	46
<i>Figure 21: Undertray integration plan.....</i>	47
<i>Figure 22: Undertray flange options .....</i>	48

## List of Figures (Continued)

<i>Figure 23: Flange bolt-hole locations</i> .....	50
<i>Figure 24: Undertray test sample</i> .....	52
<i>Figure 25: Layup schedule used for c-Car flanges</i> .....	53
<i>Figure 26: Layup schedule used for e-Car flanges</i> .....	54
<i>Figure 27: Undertray drop link inside side-pod</i> .....	55
<i>Figure 28: Undertray splitter with mounting brackets</i> .....	56
<i>Figure 29: Layup schedule for splitter flat-plate</i> .....	57
<i>Figure 30: Splitter mounting brackets</i> .....	58
<i>Figure 31: Mechanical design of undertray</i> .....	58
<i>Figure 32: Undertray mold initial design iteration</i> .....	61
<i>Figure 33: Undertray mold final design iteration</i> .....	61
<i>Figure 34: Undertray joggle mold on the top half mold</i> .....	62
<i>Figure 35: Close-up of undertray joggle mold on the top half mold</i> .....	62
<i>Figure 36: Joggle mold remodeled to generate G-code easier</i> .....	62
<i>Figure 37: Wing Insert Mold first design concept</i> .....	63
<i>Figure 38: Wing Insert Mold final design concept</i> .....	64
<i>Figure 39: Undertray endplate mold first design concept</i> .....	64
<i>Figure 40: Undertray endplate mold final design concept</i> .....	65
<i>Figure 41: Top Flange Mold initial design concept</i> .....	66
<i>Figure 42: Undertray Top Flange Mold final design concept</i> .....	67
<i>Figure 43: Bottom flange mold initial design concept</i> .....	68
<i>Figure 44: Bottom flange mold final design concept</i> .....	68

## List of Figures (Continued)

<i>Figure 45: Stock for top and bottom mold sized in CAD</i> .....	72
<i>Figure 46: Making the stock for the undertray airfoil section molds</i> .....	72
<i>Figure 47: Roughing and finishing passes for undertray molds</i> .....	74
<i>Figure 48: Cleaning and covering the CNC machine</i> .....	74
<i>Figure 49: Machining the joggle and top half undertray mold</i> .....	74
<i>Figure 50: Filling in gaps in the mold with REN-Weld</i> .....	75
<i>Figure 51: The finished and sealed undertray molds</i> .....	75
<i>Figure 52: Making the stock for the wing insert molds</i> .....	76
<i>Figure 53: Profiling tool path for one of the undertray wing insert parts</i> .....	77
<i>Figure 54: Dialing in the right feeds and speeds for machining MDF</i> .....	77
<i>Figure 55: Wing insert molds after being machined</i> .....	78
<i>Figure 56: Undertray wing insert puzzle piece connection</i> .....	78
<i>Figure 57: Sealing wing insert molds</i> .....	79
<i>Figure 58: Finished undertray wing insert mold</i> .....	79
<i>Figure 59: Profiling tool path for the undertray endplate mold back piece</i> .....	80
<i>Figure 60: Undertray endplate mold machining mistake</i> .....	80
<i>Figure 61: Undertray endplate mold after being glued and sanded</i> .....	81
<i>Figure 62: Failed attempt at sealing the surface of the MDF board</i> .....	81
<i>Figure 63: The stock for the top flange mold sized in CAD</i> .....	82
<i>Figure 64: Making the stock for the flange molds</i> .....	82
<i>Figure 65: Tool path for the finishing pass of the bottom flange mold</i> .....	83
<i>Figure 66: Machining the top flange molds</i> .....	83

## List of Figures (Continued)

<i>Figure 67: Finished undertray top flange mold together</i> .....	84
<i>Figure 68: Finished undertray bottom flange mold</i> .....	84
<i>Figure 69: Undertray carbon fiber and core templates</i> .....	85
<i>Figure 70: Layup of the undertray airfoil section</i> .....	86
<i>Figure 71: Creating the joggle on the top half undertray airfoil section</i> .....	87
<i>Figure 72: Vacuum bagging the undertray bottom mold</i> .....	87
<i>Figure 73: Both sides of the undertray airfoil section</i> .....	88
<i>Figure 74: Wing halves connected at the leading edge with the joggle</i> .....	88
<i>Figure 75: Carbon fiber backing used as a template</i> .....	88
<i>Figure 76: Front wing insert being laid up</i> .....	89
<i>Figure 77: All the wing inserts for one aerodynamics package</i> .....	89
<i>Figure 78: T800 PW 1/4-inch hard-point plate</i> .....	90
<i>Figure 79: The hard-point plate inside Edge-CAM</i> .....	90
<i>Figure 80: Water-jetting the hard-point plate</i> .....	91
<i>Figure 81: Finished hard points</i> .....	91
<i>Figure 82: Using the undertray endplate mold to cut the core</i> .....	92
<i>Figure 83: Finished and sealed undertray endplate</i> .....	93
<i>Figure 84: Layup of the c-Car undertray top flanges (with core gussets)</i> .....	93
<i>Figure 85: Finished c-Car undertray flanges</i> .....	93
<i>Figure 86: Layup of the e-Car undertray top flanges (no core)</i> .....	94
<i>Figure 87: MDF spar and gurney flap molds</i> .....	94
<i>Figure 88: Splitter flat plate template</i> .....	95

## List of Figures (Continued)

<i>Figure 89: Splitter flat plate layup process .....</i>	95
<i>Figure 90: Bottom of cured splitter flat plate .....</i>	96
<i>Figure 91: Curved aluminum sheet metal used as molds for the curved panels .....</i>	96
<i>Figure 92: Cured panels of the splitter.....</i>	96
<i>Figure 93: Side-view of preliminary assembly of the undertray .....</i>	97
<i>Figure 94: Undertray trimming templates.....</i>	97
<i>Figure 95: Process used to get straight edge for cutting.....</i>	98
<i>Figure 96: Sanding down to the masking tape .....</i>	99
<i>Figure 97: Weld-nuts located using endplate .....</i>	99
<i>Figure 98: Bonding the Undertray Airfoil, Spar, and Wing Insert .....</i>	100
<i>Figure 99: Undertray Locater Template .....</i>	101
<i>Figure 100: Marking the location of the flanges .....</i>	102
<i>Figure 101: Bonding the flanges to the undertray.....</i>	102
<i>Figure 102: Gluing potted inserts into the chassis for the undertray.....</i>	103
<i>Figure 103: Before and after the potted inserts were glued in.....</i>	103
<i>Figure 104: Side-view of undertray on chassis .....</i>	103
<i>Figure 105: Gurney flap taped to undertray .....</i>	104
<i>Figure 106: Drop links for the undertray .....</i>	104
<i>Figure 107: Drop link on the undertray and chassis.....</i>	104
<i>Figure 108: Brackets epoxied to splitter flat plate .....</i>	105
<i>Figure 109: Splitter panel template .....</i>	106
<i>Figure 110: Finished splitter with panels.....</i>	106

## List of Figures (Continued)

<i>Figure 111: Car speed data during coast-down testing .....</i>	109
<i>Figure 112: Pressure taps connected to the differential pressure sensor .....</i>	110
<i>Figure 113: Static pressure tap and Pitot tube on top of the roll hoop.....</i>	110
<i>Figure 114: Differential pressure and speed raw data .....</i>	110
<i>Figure 115: Undertray pressure gradient from CFD.....</i>	111
<i>Figure 116: Pressure gradient for 45 KPH.....</i>	112
<i>Figure 117: Pressure gradient for 45 KPH with undertray .....</i>	112
<i>Figure 118: Pressure gradient for 65 KPH.....</i>	113
<i>Figure 119: Pressure gradient for 65 KPH with undertray .....</i>	113
<i>Figure 120: Pressure gradient for 80 KPH.....</i>	113
<i>Figure 121: Pressure gradient for 80 KPH with undertray .....</i>	114
<i>Figure 122: Broken undertray wing insert replaced with steel tab.....</i>	116
<i>Figure 123: Leading edge damage .....</i>	116
<i>Figure 124: M6 flanged potted insert for the drop link.....</i>	117

## LIST OF TABLES

<i>Table 1: 2012 Undertray (UT_GFR12) vs. 2013 Undertray Baseline (A_1)</i> .....	28
<i>Table 2: 2013 Undertray Aerodynamic Specifications</i> .....	34
<i>Table 3: Carbon Fiber Materials Available</i> .....	35
<i>Table 4: Adhesives Available</i> .....	35
<i>Table 5: Undertray Mass Estimate</i> .....	59
<i>Table 6: Mold Materials Available</i> .....	60
<i>Table 7: Undertray Parts List</i> .....	69
<i>Table 8: Actual Undertray Mass</i> .....	115

## **1. INTRODUCTION**

The Formula Society of Automotive Engineers (SAE) Series are international design competitions that challenge teams of university students to conceive, design, fabricate, develop, and race a small, formula style vehicle. Each team must follow the Formula SAE Rules, but the overall design of the vehicle is very open to allow for greater creativity and innovation [1]. At competitions, the cost, presentation, and design of the vehicle is evaluated during “static events”, while the performance is assessed in “dynamic” events. The goal of the competition is to promote excellence in engineering by allowing students to apply textbook theory to real work experiences.

In 2010, the Beaver Racing Team of Oregon State University (OSU) and the BA Racing Team of Duale Hochschule Baden-Wurttemberg-Ravensburg (DHBW-R) merged into a single competing entity, Global Formula Racing (GFR). This is the first international collaboration in the history of both the US and European Formula SAE programs. This partnership allows GFR to build two cars every year (combustion and electric), and race at events in both the United States of America and Europe.

Observation of Formula SAE design trends [2] and a student-built lap time simulation coupled with the Formula SAE scoring model have revealed the high importance of aerodynamic downforce to overall competition points. As a result, significant progress has been made in recent years to develop an effective aerodynamics package for the GFR vehicle, mainly using computational fluid dynamic (CFD) simulations validated by physical testing. For this current 2013 season, GFR sought to manufacture an aerodynamics package for both the combustion car (c-Car) and electric

car (e-Car) for the first time. The package includes a front wing, rear wing, undertray, and windshield gurney for both cars, and side-pods for the c-car.

This thesis will focus on the development of the undertray for the 2013 aerodynamics package, including the aerodynamic design, the mechanical design, the manufacturing, and the physical validation.

## 2. BACKGROUND

Section 2 will provide a brief overview of relevant background material. Additional information can be found in the cited resources.

### 2.1. Aerodynamics

A racecar uses aerodynamic downforce for greater traction during acceleration, braking, and cornering. This often leads to significantly faster lap times, making aerodynamics a very important aspect of vehicle design.

#### 2.1.1. Underbody Aerodynamics

The exploitation of underbody airflow with an undertray to create downforce facilitated the “proverbial giant leap” in competition car performance [4]. The main advantages of an undertray, in comparison to wings, include the high efficiency and the increased presence of ground effect from the close proximity to the ground [5]. The idea behind the modern undertray is to use the underbody and the ground to create a Venturi. Most undertrays have a converging inlet that increases the velocity of air, a throat section where the maximum velocity is maintained, and then a diverging diffuser where the air is decelerated back down to free stream velocity. In the throat section, the high velocity results in a low pressure region that creates a net downward force. Inlet angle, diffuser angle, ground clearance, and interaction with the front and rear wing all play a role in the performance of an undertray [4, 5]. While history has shown that undertrays can be shaped to create a large amount of downforce, a large database of information on designs does not exist (as it does with airfoils), making the design process more challenging [4].

### **2.1.2. Computational Fluid Dynamics**

Computational fluid dynamics (CFD) software can be used to estimate the aerodynamic performance (i.e. pressure, velocity, downforce, drag, etc.) of a vehicle through numerical methods and algorithms. This is done by importing the car model from a Computer Aided Design (CAD) package, putting it within a test block (a virtual wind tunnel), meshing the surface into many cells, and then allowing the software to numerically solve each cell using given physics parameters and mathematical models. Using CFD allows for a large number of designs to be tested, but achieving accurate results can be difficult due to all the small details that must be fine-tuned. Nonetheless, students have used CFD to design Formula SAE vehicles before with much success [6]. STAR-CCM+ by CD-adapco will be the CFD software used, while CATIA V5 will be the CAD software used.

### **2.1.3. Physical Testing**

A number of physical tests can be performed to validate the aerodynamic design of a vehicle on-track. The most obvious and simple test is “on-off” lap time testing where the vehicle does laps with the aerodynamic devices on, and then does laps with the aerodynamic devices off to see if the vehicle is indeed faster with aero. Other tests to learn more about the aerodynamic behavior of the vehicle include flow visualization, pressure tapping, coast-down testing, and strain gauging. Off the track, the vehicle or a scale model of the vehicle can be put into a wind tunnel for a much more controlled test. However, a ground rolling wind tunnel is often necessary to produce accurate results.

## **2.2. Carbon Fiber Manufacturing**

With its extremely high strength to weight ratio, carbon-fiber-reinforced polymer (CFRP or simply carbon fiber) is a common composite material selected for racecar parts [7]. This is especially true for aerodynamic devices, which need to be lightweight to ensure their mass does not offset their aerodynamic gains.

### **2.2.1. Pre-Impregnated Carbon Fiber**

Pre-impregnated carbon fiber, or prepreg, is a type of carbon fiber where the resin is already precisely wetted into the fibers. This requires prepreg carbon fiber to be stored in a refrigerator to prevent premature curing of the resin, but greatly increases the ease of fabrication by eliminating the complications associated with wet resin [8]. The molder only needs to lay the prepreg sheets on the mold, remove the air with a vacuum bag, and then place the part in an oven to cure.

### **2.2.2. Sandwich Structures**

While carbon fiber laminates are very strong in the X and Y directions, they have much less strength and stiffness in the Z direction (e.g. from bending). To address this problem, the most common solution is a sandwich structure that consists of a core glued in between two carbon fiber face sheets. The sandwich panel increases bending stiffness by allocating most of the strength away from the neutral axis where the normal stress from bending is the largest, similar to an I-beam. While incorporating core increases the complexity of the part for a number of reasons, the substantial gain in bending strength and stiffness with minimal gain in mass is highly advantageous.

### **2.2.3. Composite Design**

Composite structures are much more difficult to design than single-phase structures (e.g. most metals, plastics, and ceramics) because they are anisotropic, have constituents with varying influences, are more challenging to manufacture, and have a variety of failure modes [8]. It is also more difficult to accurately simulate the mechanical performance of composite structures using finite element analysis (FEA). As a result, an understanding of the material behavior and an awareness of the many variables associates with the design of composites is often required to successfully design composite structures. This knowledge is best gained from manufacturing a number of test samples to experiment with different layup schedules.

### 3. CONCEPTUAL DESIGN

Section 0 will detail the initial design phase of the 2013 undertray, which includes an overview of the engineering requirements, an analysis of the current state for benchmarking purposes, and the initial concept.

#### 3.1. Requirements

##### 3.1.1. General Quantitative Requirements

The most important requirement for this aerodynamics package is the maximization of competition points. If it does not make the team more competitive, it should not go on the car. In order to satisfy this primary requirement, the aerodynamics package must meet the following general criteria:

- **High downforce:** Downforce improves cornering speeds and as a result, lap times. This is especially true for Formula SAE, where the course tends to be traction limited as opposed to power limited [2].
- **Low drag:** Drag creates unwanted frictional forces that limit top speed and reduces fuel efficiency. Gains in downforce are usually coupled with losses from drag.
- **Lightweight:** GFR's lightweight vehicle concept has yielded much success in recent years. If aerodynamic elements are to be integrated, a lightweight design will be required. Reductions in weight also lead to less moment of inertia, which will lower resistance to rapid changes in direction. To achieve a

lightweight design, a solid integration plan must be developed since a lot of weight can be added from impromptu mounting ideas.

### 3.1.2. Formula SAE Competition Requirements

Since the car must compete in a number of different events, it is important to understand which requirements are the most important for each event. The following explains the requirements of the aerodynamics package for each Dynamic Event:

- **Dynamic Events (675 Points Total)**

- **Acceleration (75 Points):** The aero package must be *lightweight* to increase acceleration potential, along with *low-drag* to reduce impediment of forward movement. If properly designed, the aerodynamics package should result in similar or marginally slower times [2].
- **Skid-Pad (50 Points):** The aero package must be *lightweight* to increase lateral acceleration, and be adjustable to a *maximum downforce* position since acceleration and top speed are insignificant factors in scoring well. An aerodynamics package should result in similar or marginally faster times [2].
- **Autocross (150 Points):** Autocross requires an aero package that is *lightweight*, has *high downforce*, and relatively *low-drag*. An aerodynamics package will lead to slower straight-line acceleration, significantly higher cornering potential, similar to higher yaw acceleration potential, higher slalom speeds, and significant higher braking potential [2].

- **Endurance (300 Points):** The aero package must be *lightweight*, have *high downforce*, and *low-drag* to ensure fast laps during the Endurance event. The gains and losses of an aerodynamics package will be the same as those for Autocross [2].
- **Efficiency (100 Points):** A *lightweight* and *low-drag* aerodynamic package will reduce the fuel consumption, but not as much as if there was no aerodynamics package. Therefore, a sufficient trade-off point should be determined.

Clearly, the design of an aerodynamics package for Formula SAE requires many trade studies since the effect of an aerodynamics package varies from event to event. However, this situation is simplified when the one remembers the ultimate goal: to win competitions.

### **3.1.3. Equating design parameters to points**

Since competitions are won by points and not typical racecar performance, a lap time simulations was coupled with a competition scoring model to equate design parameters (e.g. downforce, drag, mass, etc.) to points. This helps calculate how many points will be gained from downforce, how many points will be lost from drag, and which design is truly superior.

### **3.1.4. General Qualitative Requirements**

In addition to maximizing points, the following qualitative requirements must also be met:

- **Balanced center of pressure:** The center of pressure (CP), or the point through which the sum of a pressure field acts on a body, must be balanced to maintain vehicle stability. The CP will be considered a qualitative requirement because the “perfect location” for the CP is difficult to determine due to how it changes with speed (e.g. braking, acceleration) and driver preference. In general, the CP should be behind the center of gravity (CG) at average speeds so that the vehicle is inherently stable during braking when the CP moves forward. This is how regular road cars are designed. Move it too far aft though and the car tends to under steer, which limits the driver’s cornering ability. This is where driver preference comes into play, because a more experienced driver may prefer the CP more forward if he/she wants more front grip for turning and can handle the more unstable braking and sharper turning behavior. With the CG of a GFR vehicle being approximately 52 percent rearward between the wheels with a driver, the arbitrarily selected target CP range will be 55 to 65 percent for simulation purposes. However, in real life, the vehicle will still need to be tuned to match the driver’s preference and actual vehicle drivability.
- **Robust:** Since the aerodynamic devices are external of the chassis, they are the most likely to experience the impact of a cone. At high speeds, the loading can be very significant, requiring robust aerodynamic devices that can experience these forces without failing and possibly causing a disqualification during competition. This requirement will be assessed qualitatively by physical testing since simulating impacts are difficult to do accurately.

- **Easy to manufacture:** Regardless of whether the aerodynamics package looks effective during CFD simulation, the true gains will not be experienced until it is built and integrated to the vehicle. Therefore, the ability to manufacture the necessary parts easily and timely will be very important.
- **Easily integrated:** The aerodynamic components will interface with parts of many other sub-teams, including chassis, combustion powertrain, impact attenuator, and suspension/data acquisition (DAQ). Therefore, communication during the initial design phase will be very important in order to prevent conflicts down the road.

### **3.1.5. Formula SAE Rules and Requirements**

In addition to these requirements, the GFR 2013 vehicles must abide by all the rules detailed in the 2013 Formula SAE Rules [1]. The rules specific to Formula Student Germany Combustion [9] and Formula Student Germany Electric [10] must be followed as well if GFR is to compete at these competitions.

## **3.2. Initial Concept**

A new undertray design was conceived, inspired by the Lotus Type 78 F-1 car, which had side-pods with an inverted airfoil profile on the bottom, sealed off with rigid sliding seals. The new 2013 undertray concept is shown in *Figure 1*. It was chosen to have a Joukowsky airfoil with 12% thickness and 10% camber. It spans outward to the widest part of the tires (this is the limit set by the FSAE rules [1]). Air is directed to these airfoil sections by the bottom section, which will be called the splitter. The splitter also

covers up the suspension assembly underneath the vehicle, keeping the underbody flow smooth and laminar.

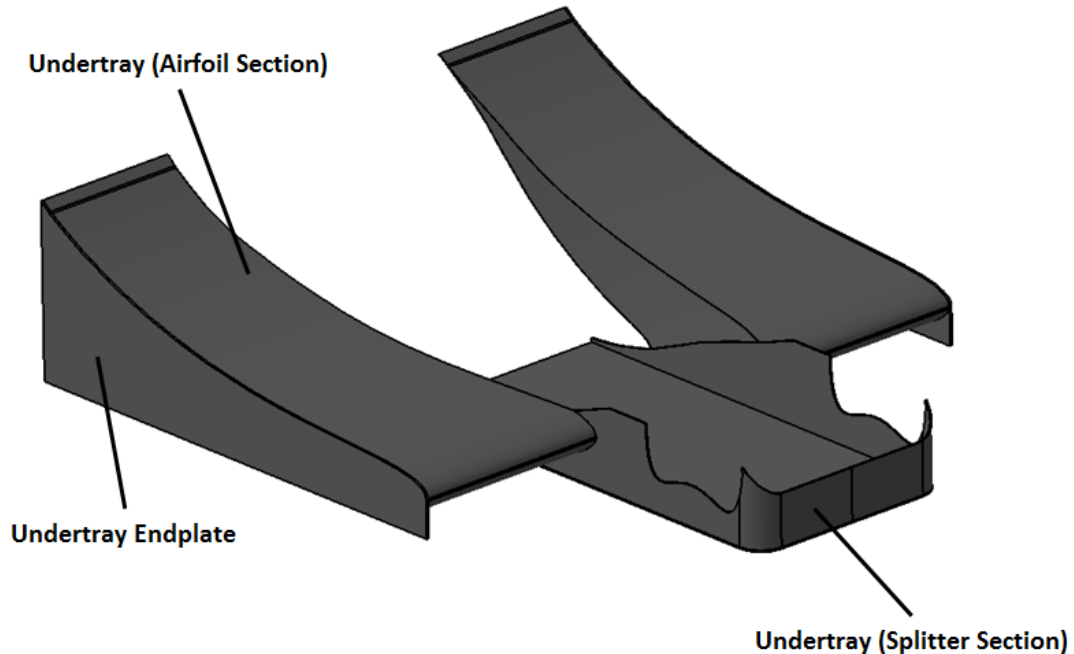


*Figure 1: GFR 2013 undertray baseline concept*

After a quick examination of this concept, the following advantages and disadvantages are apparent:

- **Advantages:**
  - **Centralized CP:** Since the CP of the airfoil is more forward and in between the wheels, this will move the global CP forward as well towards the optimal range of 55-65 percent.

- **Smaller moment of inertia:** With the diffuser section in between the tires as opposed extending aft of the tires like previous years, the resistance to changes in direction will be much less.
- **Simpler design:** Like the front wing, this is a wing in ground effect. This concept has worked in the past and the aerodynamic principles that justify it are much simpler.
- **Easier to manufacture:** Manufacturing this undertray will be very similar to manufacturing the wings, which have taken less time in the past. This should enable the production of two copies for each car.
- **Lightweight:** The design does not extend the full length of the car, and therefore requires fewer materials. This will make it significantly lighter.
- **Cheaper:** Utilizing fewer materials will decrease the cost as well.
- **Interaction with the wings:** While this is not necessarily guaranteed, the front wing could help feed air into the undertray while the rear wing could help suck air out of the diffuser.

- **Disadvantages:**

- **Higher CG:** For the c-Car, moving the side-pods (and radiators) upward and having most of the undertray not actually underneath the vehicle will raise the global CG. This will marginally increase the vehicle's tendency to roll.
- **Interaction with the tires:** Having the undertray between the tires makes it much more susceptible to the turbulence coming off of the spinning tires. Having cleaner air is obviously preferred.

- **Not modular on the c-Car:** Due to the integration with the side-pods on the c-Car, this undertray design will likely have to stay on the vehicle even if it does not work. Without side-pods on the e-car, it can be taken off.
- **Less efficiency:** Since it is not hidden underneath the vehicle and is instead extending out from the side, this undertray will likely produce more drag per unit of downforce, lowering the efficiency.

The first CFD simulation performed of the aerodynamics package with this new concept showed very promising results, which can be seen in *Table 1*.

<i>Table 1: 2012 Undertray (UT_GFR12) vs. 2013 Undertray Baseline (A_1)</i>		
<b>Benchmark</b>	<b>UT_GFR12</b>	<b>A_1</b>
Undertray Downforce	112.2 N	201.4
Undertray Drag	10.8 N	42.4
Undertray Efficiency (L/D)	10.40	4.75

## 4. AERODYNAMIC DESIGN

Section 4 details the aerodynamic design analysis of the undertray, and the iterative process used to improve its performance using CFD simulations.

### 4.1. Aerodynamic Behavior

Looking at the images from the CFD simulations, it is clear that while the undertray is an inverted airfoil profile, it still operates under the Venturi effect as opposed to wing circulation. In other words, the undertray profile converges, increasing the velocity, and then diverges, decreasing the velocity. Where the velocity is highest in *Figure 2* is where the static pressure is lowest in *Figure 3*. This lower pressure region (relative to the pressure of free stream air) is what creates the desired downward force. Having the diffuser expand gradually at the same rate as an airfoil profile seems to keep the flow attached much longer than a typical Venturi style undertray diffuser.

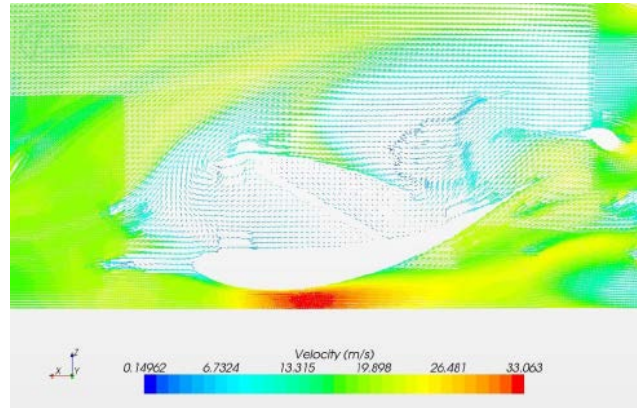


*Figure 2: GFR 2013 undertray baseline velocity vectors*

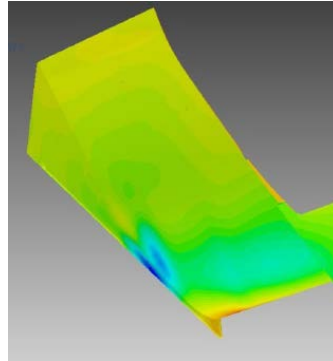


*Figure 3: GFR 2013 undertray baseline pressure gradient*

## 4.2. Undertray Additions

With such a strong baseline design, only minor changes were iterated and run through CFD. This did not include chord length, angle of attack, ground clearance, or X-location, but these would be good parameters to examine in future analyses. Minor changes that were explored include the effects of adding outer skirts, inner skirts, and tire deflectors to the undertray endplate. Gurney flaps, vortex generators, and strakes were also explored. All the case studies explored can be seen in *Figure 4*. The goal of these additions was to create more downforce and reduce drag by improving the sealing of the low pressure area, keeping the flow attached longer, deflecting the turbulence of the tires, or creating more laminar flow.

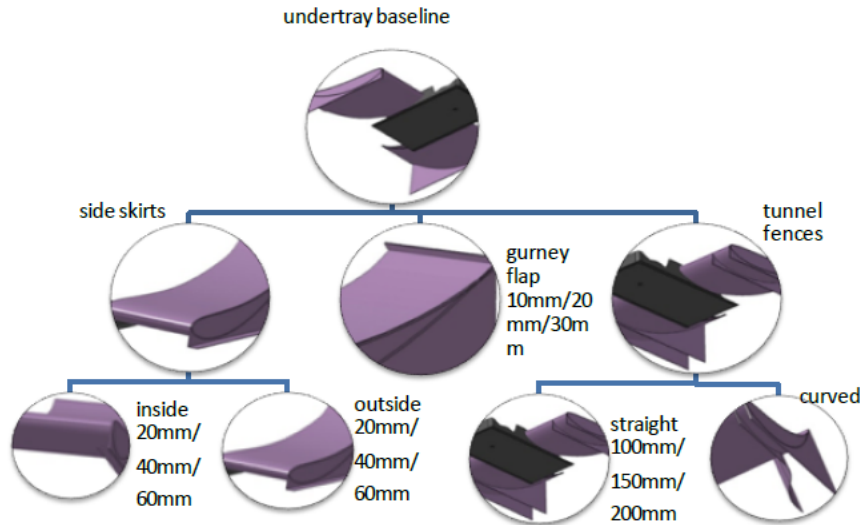


*Figure 4: GFR 2013 undertray concept*

### 4.3. Splitter Study

The original rectangular splitter (as seen in *Figure 1*) that directs the flow toward the airfoil section and covers the suspension underneath the vehicle seemed to be rather “draggy”. Therefore, a new “curvy” splitter, as shown in *Figure 5*, was tested in CFD.



*Figure 5: Curvy splitter*

The curvy splitter resulted in more total downforce, less total drag, and more total points, but not in a manner that was expected. The downforce from the undertray was reduced, but was coupled with an increase in downforce from the rear wing and a

decrease in lift from the side-pod. This may indicate that the flow remains laminar and stays attached longer resulting in cleaner air aft of the undertray and inside the side-pod. However, this is completely speculative, as it is difficult to see any difference in the streamlines. Nonetheless, the difference in points was marginal. Therefore, the rectangular splitter was chosen since it is the simpler design, is less likely to skid on the ground during braking, and does not obstruct the pedal adjustment points underneath the chassis.

Later in the design process, a 50 mm (2 in.) front lip was added to the splitter and the width of the bottom plate was extended by 19 mm (0.75 in.) on each side. The front lip was added to create more downforce, since the stagnation of the flow above the lip has high pressure and can press down on it to create more downforce. The increase in width was done just in case that area was needed for mounting to the suspension links and to account for error when locating the part on the chassis. Neither of these changes was studied in CFD. The rectangular splitter with these new changes is shown in *Figure 6*.

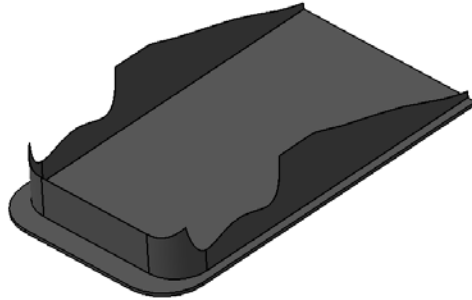


*Figure 6: New rectangular splitter*

#### 4.4. Endplate Study

A new undertray endplate similar to a concept tested successfully for the front wing was created and tested in CFD. The concept is shown in *Figure 7*. It was hoped that this new endplate design would help guide flow over the tires to reduce tire drag.

The new endplates reduced overall performance significantly by decreasing the downforce of the undertray. It is difficult to determine whether this was an error of the simulation, or if the flow coming from the side and over the undertray plays an important role and blocking off that air is counter intuitive. Either way, ST-1 was chosen because it was simple and the gains from this new endplate design (if any) would most likely be marginal. Though, studying an endplate that extends more upward like this for the e-car where there is no a side-pod would be interesting and possibly advantageous. However, there was not enough time to do so.

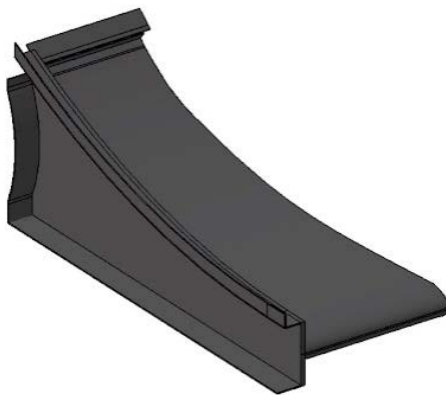


*Figure 7: Undertray with the new endplate concept*

## 4.5. Aerodynamic Design Summary

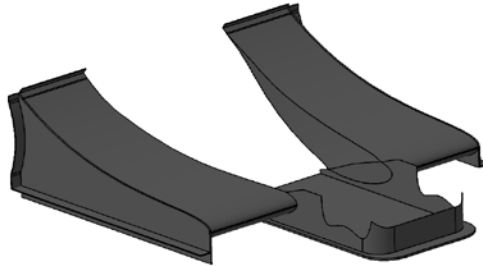


*Figure 8: Final undertray aerodynamic design*

The final undertray design, which can be seen in *Figure 8*, is the result of an iterative process where the goal was to gain competition points. Compared to the baseline, it now has tire deflectors and an outer side skirt on the endplate, and a reduced span to accommodate these additions.

Table 2: 2013 Undertray Aerodynamic Specifications		
Parameter	Value	Unit/Description
<b>Airfoil Section</b>		
Chord Length	1000	mm
Total Span	360	mm
Profile	Joukowsky	Classification
Thickness	12%	Percent of chord
Camber	10%	Percent of chord
Angle of Attack	15	degrees
<b>Add-Ons</b>		
Gurney Flap	30	mm
Outer Side-Skirt	40	mm
<b>CFD Results</b>		
Downforce	258.4 N	N
Drag	44 N	N
Efficiency	5.87	L/D

## 5. MECHANICAL DESIGN

With the aerodynamic design complete, the mechanical design and the integration plan will now be discussed. Section 5 details the number of ideas that were explored. Due to the short time constraint and the challenging manufacturing demands, the focus was on actual implementation and physical testing, as opposed to developing an optimized solution through simulation.

### 5.1. Materials Available

*Table 3* and *Table 4* list the materials that were available through sponsorship to manufacture the undertray out of carbon fiber.

*Table 3: Carbon Fiber Materials Available*

<b>Material</b>	<b>Data Sheet</b>
Toray T800H PW	[11]
Toray T800 Unidirectional	[11]
Hexcel HRH-10-1/8-3.0, ¼" thick	[12]
Hexcel HRH-10-1/8-3.0, ½" thick	[12]

*Table 4: Adhesives Available*

<b>Material</b>	<b>Data Sheet</b>
Henkel Loctite Hysol Product 9430 (cream colored)	[13]
Henkel, Loctite, Hysol Product 9380 (gray colored)	[14]

Toray T800 is an intermediate modulus, high tensile strength fiber, with excellent balanced composite properties for aerospace applications [11]. Hexcel HRH-10 is an aramid fiber honeycomb sheet for use as core material in sandwich panels [12]. To bond

the carbon fiber parts together, the available high strength adhesives available were Hysol 9430 [13] and Hysol 9340 [14].

## 5.2. Undertray Airfoil Section Structure

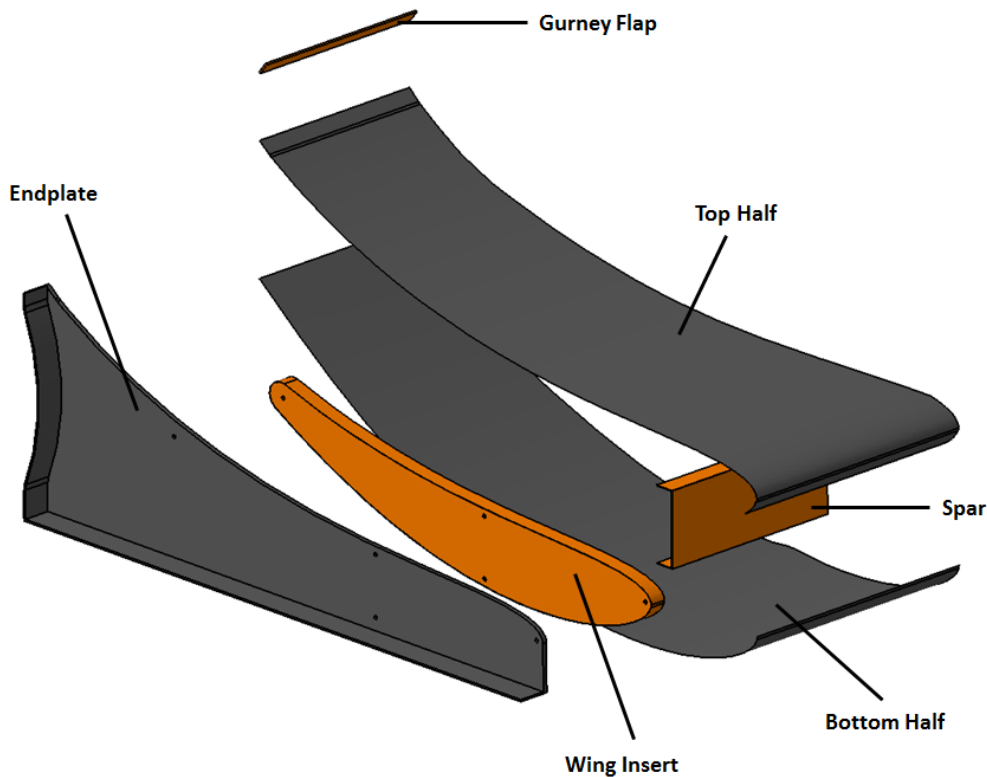


Figure 9: Undertray Airfoil Section exploded view

Since this undertray is so similar to the wings, it made sense that it would have a similar structure that included two wing halves (top and bottom), a gurney flap, a spar, an endplate, and a wing insert that interfaces with the endplate. Everything is epoxied together, except for the endplates which are each fastened onto the wing insert by four M6 aluminum bolts. The exploded view of this structure is shown in *Figure 9*.

### 5.2.1. Wing Halves

These wing halves form the airfoil section of the undertray. The side of the wing section away from the chassis is flat for the endplate, while the other side matches the contour of the chassis.

#### 5.2.1.1. Wing Halves Layup Schedule

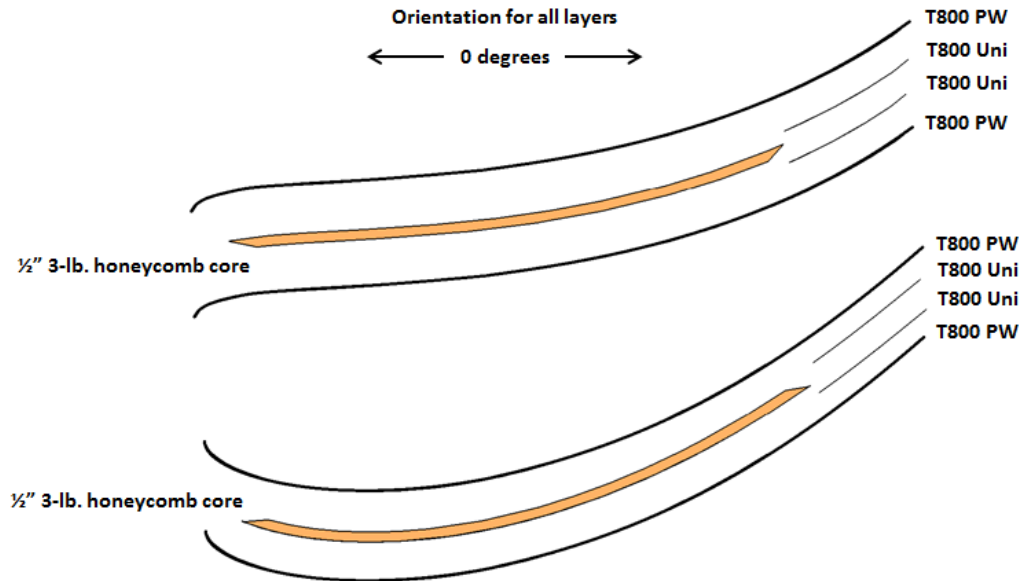
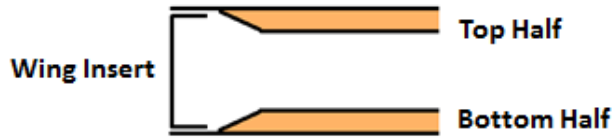


Figure 10: Side-View of the layup schedule used for undertray airfoil sections

These wing halves only need to have sufficient rigidity to not deform under impacts or aerodynamic loads. Therefore, to obtain this rigidity and keep it as lightweight as possible, a “1-core-1” sandwich structure was proposed based on the results of past test samples. T800 plain weave (PW) was chosen as the carbon fiber because it was readily available, while Hexcel HRH-10-1/8-3.0 ½-inch thick aramid honeycomb core was selected over the ¼-inch thick core due to the large scale of the part. Core obviously

cannot extend throughout the entire part, so the shape of the core was drawn in CAD to ensure that the core covered as much area of the undertray as possible without interfering with the wing insert, trailing edge, and leading edge. To allow for error, a tolerance of 10 mm was added.

It was later discovered that without the core, the trailing edge with only two plies of PW carbon fiber was too flimsy. Therefore, two layers of T800 unidirectional carbon fiber were laid up in between the T800 PW layers for extra reinforcement. This layup schedule used for the airfoil section of the undertray is shown in *Figure 10*. A front cross-sectional view of how the core on the top and bottom half of the undertray tapers off to leave room for the wing insert is shown in *Figure 11*.



*Figure 11: Front-view cross section of the undertray airfoil sections*

#### 5.2.1.2. Wing Halves Bonding Areas

To bond these two wing halves together, areas in the trailing edge and leading edge need to be designed for bonding. Thus, for the trailing edge, the bottom contour of the airfoil was offset upward 1.5 mm and joined with the top contour of the airfoil in the CAD model. This created a region for bonding where the bottom and top are parallel, as shown in *Figure 12*, instead of coming together to a finite point. The offset was set to 1.5

mm because 4 plies of cured T800 PW were measured to be about 0.75 mm, and a bond gap of about 0.75 mm (0.030 in.) is fairly standard.

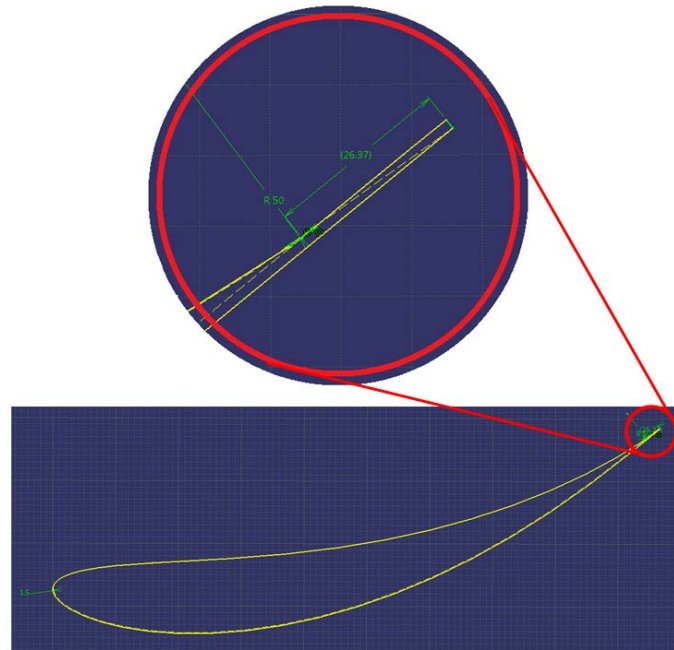


*Figure 12: Trailing edge bonding area*

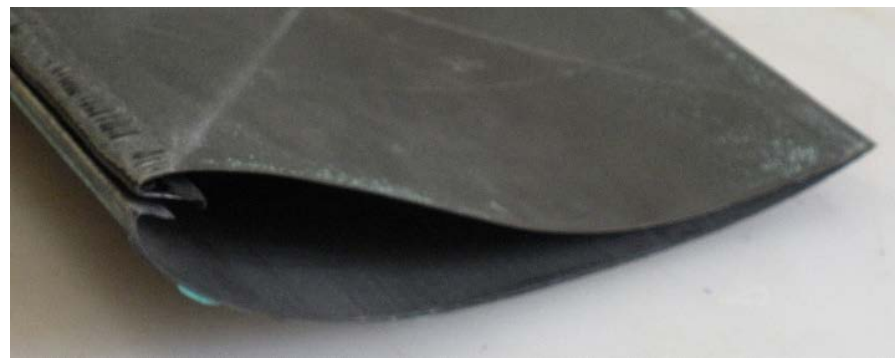


*Figure 13: Two wing halves joined together by a butt joint*

For the leading edge, the current wing molds use a butt joint as shown in *Figure 13*. This results in an undesirable gap on the leading edge, regardless of how well it is done. There have also been a lot of problems with bridging in that tight corner that result in a warped leading edge. Lastly, since each wing half needs a butt joint, each wing half mold needs also needs a butt joint mold. This means that if there is only one butt joint mold, the two wing halves must be cured separately. This increases the manufacturing time significantly.

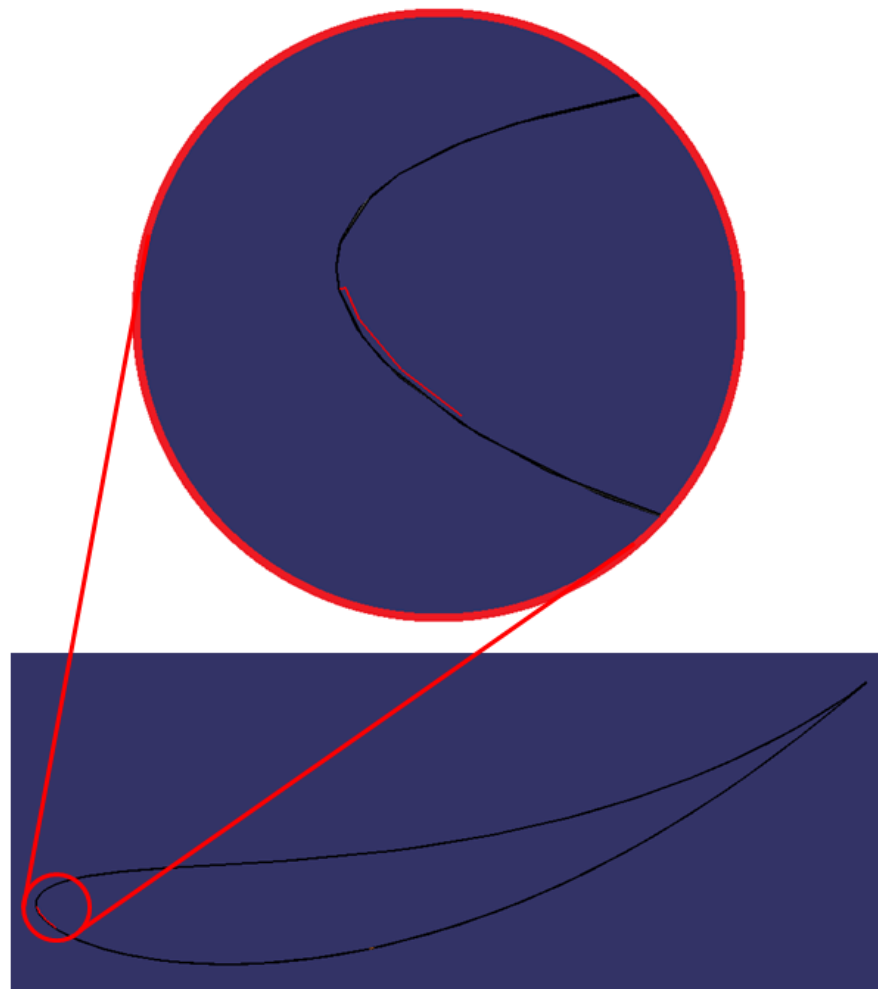


*Figure 14: Joggle concept for bonding the two wing halves together*

Therefore, a new joggle concept (inspired by how Lancair International, Inc. manufactures their wings) was designed, which can be seen in *Figure 14*. The top half of the wing extends into the bottom half so that they can be bonded together at the leading edge. The gap for the joggle was set to 1.25 mm because 2 plies of cured T800 PW is about 0.50 mm, while a bond gap of about 0.75 mm (0.030 in.) is fairly standard. This design will hopefully lead to a clean looking leading edge that will be easier to manufacture since there are no sharp, hard-to-reach corners. Also, only one of the two wing-half molds needs to have a joggle mold, allowing both to be cured simultaneously with only one joggle mold. The top half was chosen to have the joggle since it would have less curvature and would therefore be marginally easier to manufacture than if it were done the opposite way.

### 5.2.2. Gurney Flap

The gurney flap is a very simple part that will be added to the trailing edge of the airfoil section for aerodynamic purposes (i.e. more downforce).

#### 5.2.2.1. Gurney Flap Layup Schedule

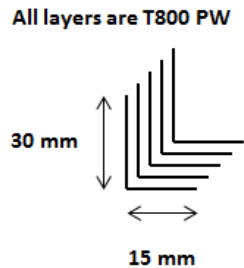


*Figure 15: Layup schedule used for gurney flaps*

Core cannot be used in this thin part. Therefore, 5 plies of T800 PW carbon fiber will be used to obtain the necessary rigidity, as shown in the layup schedule in *Figure 15*. The 15 mm side of the gurney flap will be epoxied or taped to the trailing edge of the wing section.

### 5.2.3. Spar

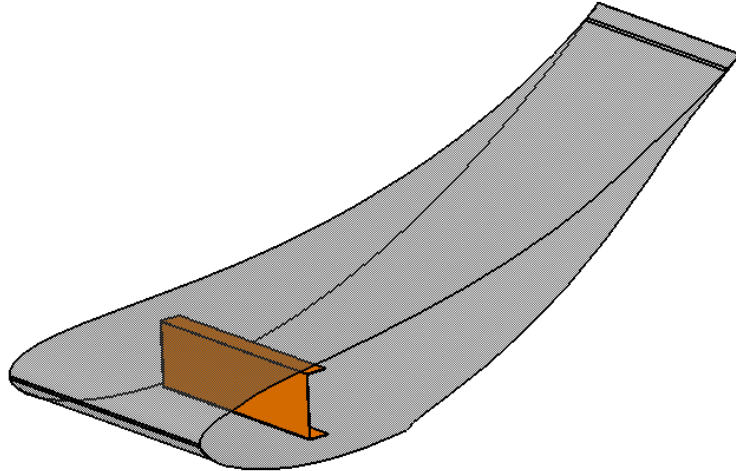


*Figure 16: Undertray spar*

The spar will support all the compressive loads of the undertray. It will be in the shape of a “C” for manufacturing purposes (i.e. the mold will be a simple bar). Other options included an “I” spar (good for bending) and an “S” spar (fits better inside the curvature of the wing profile).

The height in between the two wing halves minus the  $\frac{1}{2}$ -inch core on each side at approximately 25 percent chord length (where it was about the thickest) was measured in CAD for the height of the spar. In this case, the height of the spar was approximately 85

mm (3.35 in.). The eventual location of the spar will be determined by sliding the spar along the inside of the undertray and seeing where it fits best for bonding.

#### 5.2.3.1. Spar Layup Schedule

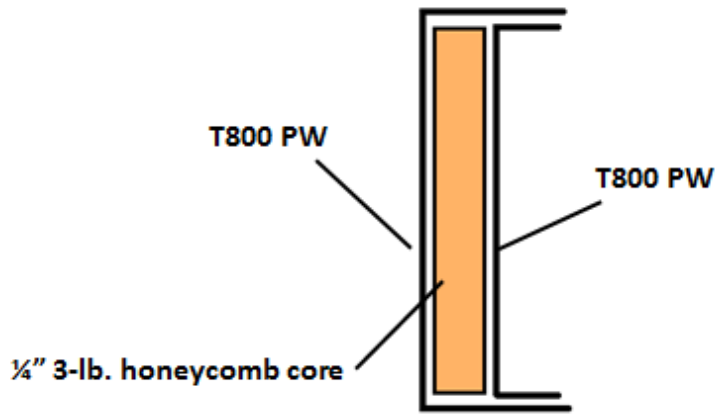


Figure 17. Layup schedule used for spars

The compressive forces will not be significant, and the spar essentially just needs to remain rigid and not buckle. Therefore, a “1-core-1” sandwich structure was proposed once again using T800 PW and  $\frac{1}{4}$ ” honeycomb core, as shown in *Figure 17*.

#### 5.2.4. Endplate

The endplate matches the contour of the airfoil on top and extends down 2.5mm below the lowest point of the airfoil to separate the low pressure region from the free stream air. There is also a cutout in the rear to ensure it does not enter the Keep-Out-Zone specified in the FSAE rules.

#### 5.2.4.1. Endplate Layup Schedule

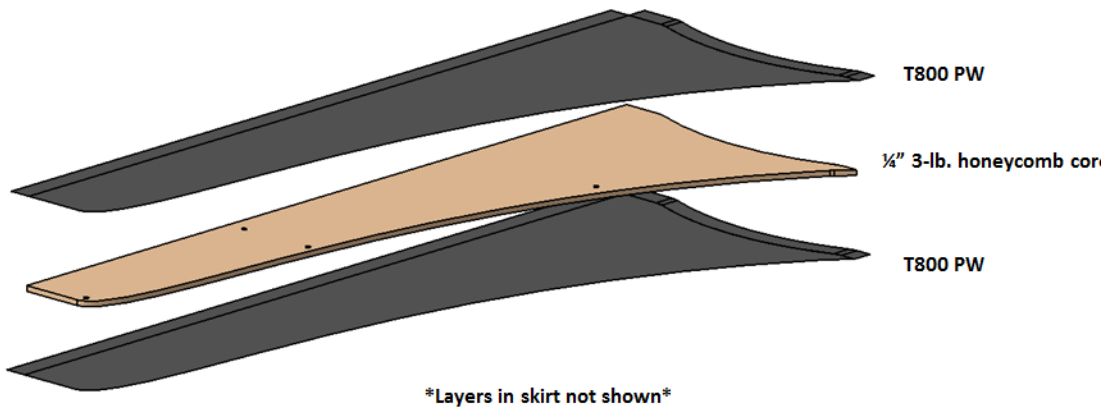


Figure 18: Layup schedule used for undertray endplates

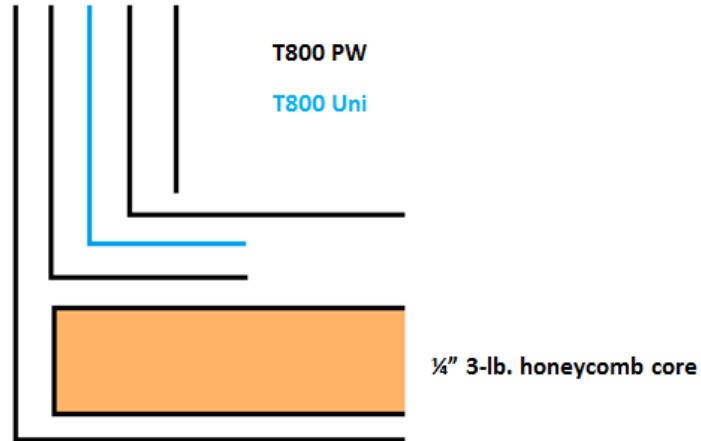


Figure 19: Layup schedule used for undertray endplate skirts

The endplate will not experience any significant loads except for some cone impacts that graze the front of it. Therefore, to get the rigidity and keep it lightweight, the endplate is also “1-core-1” using T800 PW and 1/4-inch honeycomb core. There will be 1/4" thick carbon fiber hard-points where the bolts are to prevent the core from getting

crushed. This layup schedule is shown in *Figure 18*. For the outer side skirt and tire deflector, there will be 5 layers total, with 4 of the layers supporting the right angle and 1 continuous layer on the exterior for aesthetic reasons, as shown in *Figure 19*. While on the lightweight side, this layup schedule for the skirt should support minor loads from being stepped on and being grazed by cones.

### 5.2.5. Wing Inserts

The wing insert will connect the wing halves to the endplate. It extends to 75 percent of the chord length where it is rounded off. The shape matches the exact contour of the airfoil, except it is offset inward 2.5 mm. 2 plies of carbon fiber and a sufficient bond gap is about 1.25 mm, but it was decided to double the offset to 2.5 mm to make sure the wing insert fitted inside the two wing halves. Also, a female mold will be used to make this part and sanding it may take off a few millimeters.

Wing inserts from 2011 were rapid prototyped. As a result, they were very strong, but expensive, heavy, and only a certain amount could be made. This year, to make it lightweight and relatively inexpensive, it was decided to manufacture them in-house out of carbon fiber. Also, if any of them broke, making another one would be a possibility. The threads for the fasteners will be provided by weld nuts epoxied onto the other side.

#### 5.2.5.1. Wing Insert Layup Schedule

The main compressive support for the undertray will come from the spar. So while the wing insert looks like it could be a structural rib, it was decided to make the wing insert out of only two layers of T800 PW carbon fiber. It was important to keep this

lightweight since it was such a large part. A failure mode where the endplate would be hit and rip out the wing insert was considered, but there is no real place on the endplate for a cone to grab on. Also, the epoxy that will be used to bond the wing insert to the wing halves will be very strong. The layup schedule for the wing insert is shown in *Figure 20*. Once the wing inserts are made, “windows” will be cut out where there are no weld nuts to reduce weight even further.

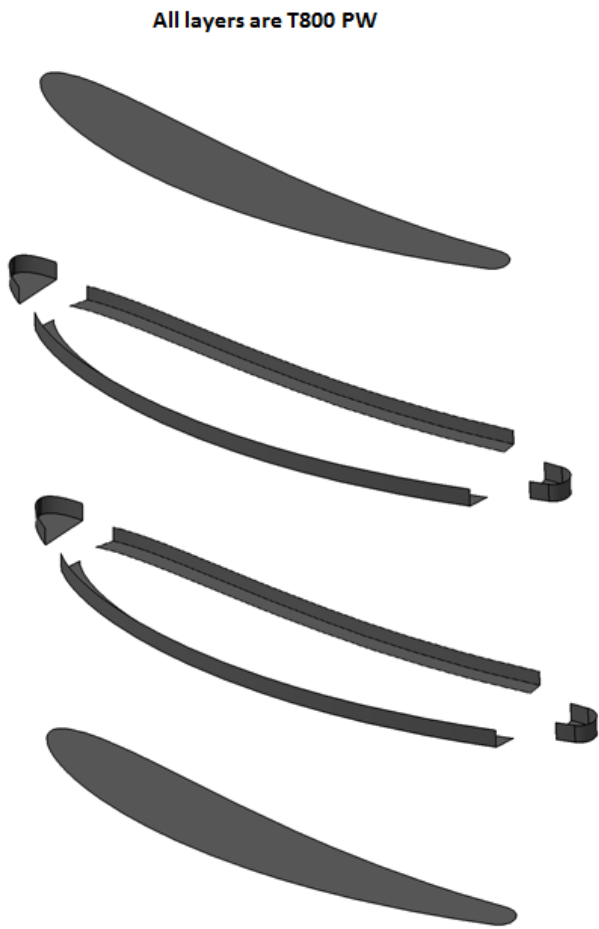


*Figure 20: Layup schedule used for the wing inserts*

### 5.3. Undertray Integration

The integration of the undertray must provide accurate positioning alongside the chassis to ensure it does not enter the Keep-Out-Zone around the tires. The mounting must also be capable of supporting the maximum amount of downforce and drag with minimal deflection to ensure the downforce is transferred to the springs of the vehicle. Lastly, it will need to be compatible with the side-pods and radiators on the c-car, and be removable for the e-car just in case it does not work (whether the undertray works or not on the c-car, it will most likely have to stay on because the side-pod will be L-bracketed to it and the chassis). It was decided that the best way to meet these requirements was to have structural carbon fiber L-brackets on the top and bottom that conformed to the shape of the undertray and chassis. An additional drop link would extend from the chassis to the outside of the undertray for extra reinforcement. The undertray structure with the integration plan can be seen in *Figure 21*.

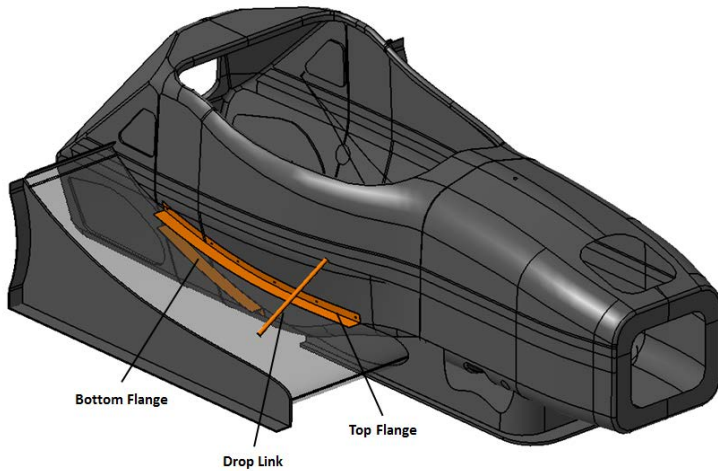


*Figure 21: Undertray integration plan*

### 5.3.1. Flanges

There are two different methods of making the undertray removable with this design: (1) bond flange to chassis, fasten undertray to flange and (2) bond flange to undertray, fasten undertray to chassis. These options can be seen in *Figure 22*.

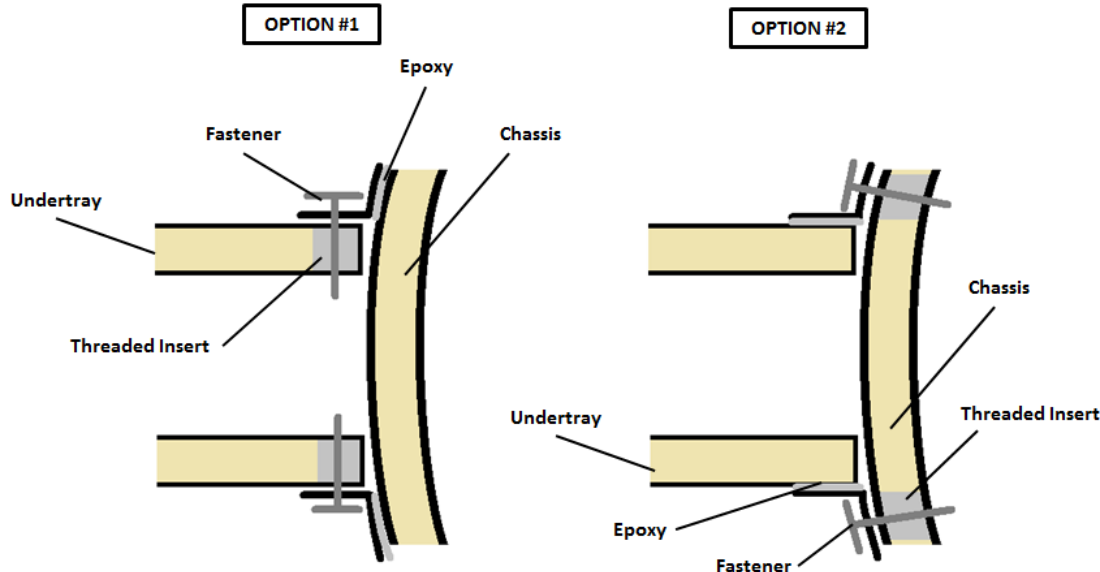


*Figure 22: Undertray flange options*

To assess these two options, it was assumed that the epoxy, the bolts, and the threaded inserts have much higher factors of safety in comparison to the flange and the undertray parts. Both options require a permanent alteration to the chassis that requires close collaboration with the chassis team. However, Option 1 results in the undertray and flange both having failure points, since there is a chance that the fastener can shear out of either of them. In Option 2, the undertray transfers the entire load to the flanges because

after bonding they essentially become one continuous structure. Option 2 also has the following advantages:

- Requires aluminum potted inserts to bonded inside the carbon fiber chassis, which has been done many times before
- Preparing the 2D undertray surface for secondary bonding with the flange will most likely be easier than preparing the 3D surface of the chassis for bonding
- Upon removal of the undertray, the flanges come off as well, leaving a clean looking chassis (aside from the visible potted inserts); this makes the undertray modular for the e-Car
- It is easier to manufacture a flange with increased area for bonding along the 2D surface of the undertray, than the 3D surface of the chassis

Due to these advantages, Option 2 was chosen. In other words, the flange will be bonded to the undertray and the bonded undertray assembly will be bolted to the side of the chassis into threaded inserts epoxied into the chassis.

#### *5.3.1.1. Flange Bonding Area*

Hysol 9380 [13] (gray colored) and Hysol 9340 [14] (cream colored) were two general purpose adhesives available at the time. Both have very high peel and shear strength. If bonded correctly, the flange will fail a lot sooner than the epoxy. Therefore, the width of the flanges along the undertray is only about 25 mm (1 inches), since the weight of epoxy can add up quickly.

### 5.3.1.2. Flange Bolt hole locations

*Figure 23* shows the flanges with a number of bolt location choices. It is important to note that while *Figure 23* shows the top and bottom flange to be continuous, they will each be broken up into two so that if the front rips off, the back will hopefully still be attached. Also, the flanges need to be broken up to leave room for the pipe going into the radiator for the c-Car, also shown in *Figure 23*.

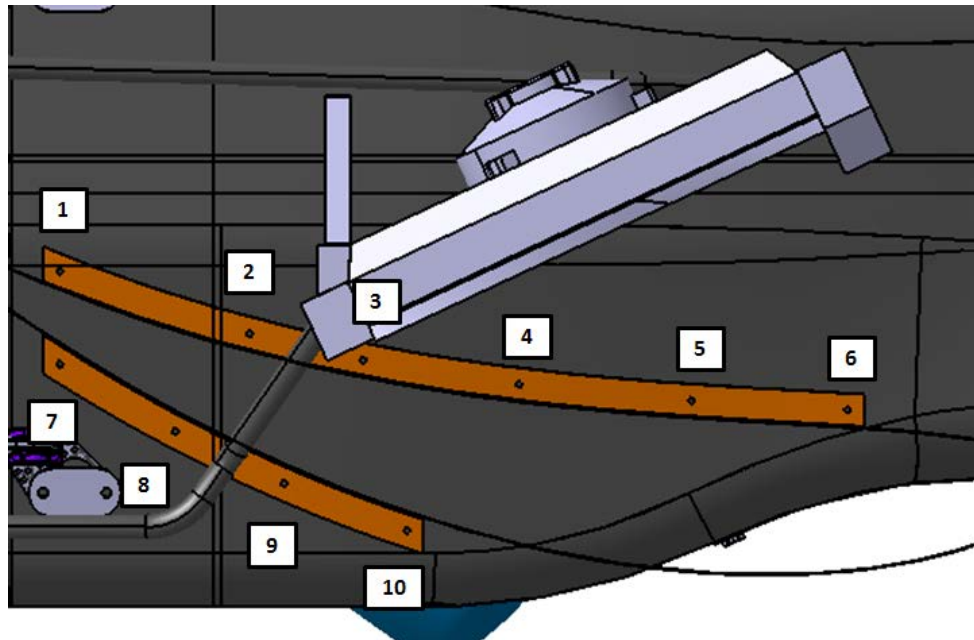


*Figure 23: Flange bolt-hole locations*

To reduce the load on each bolt, a high number of small (M4) fastening points were desired to distribute the load more evenly. However, adding more fastening points increases the weight of the vehicle. Therefore, the amount of fastening points allowed by GFR leadership was eight. For the c-Car, the top-back flange will have 2 bolt holes (1 and 2 in *Figure 23*), while the top-front flange will have 4 bolt holes (3, 4, 5, and 6 in

*Figure 23*), since it is relatively long and is more important than the bottom flange since it reaches more forward. This leaves only 2 bolts for a single bottom flange (7 and 8 in *Figure 23*). For the e-Car, there are no radiator pipes to worry about. Therefore, the top and bottom flange will each be split into two with each having two bolt holes. The top flange will be split between 3 and 4 in *Figure 23* (and omit 2, 4, and 5), while the bottom flange will be split between 8 and 9 in *Figure 23*. These bolts will fasten into aluminum M4 potted threaded inserts epoxied inside the chassis. Inserting a helical insert with steel threads into the aluminum insert to prevent stripping of the aluminum threads was considered. However, if the threads did strip, then the inserts could just be tapped again with a larger size. This would be impossible with a steel helical insert used.

#### 5.3.1.3. Test Sample

In order to get a qualitative assessment of this integration plan, a simple test sample was made, as shown in *Figure 24*. The airfoil sections and the wing insert followed the layup schedule as described in 5.2.1.1 and 5.2.5.1 respectively. The flanges were simple L-brackets made from 3 plies of T800 PW and glued to the airfoil sections. The goal was to use the test sample as a baseline to come up with a layup schedule for the flanges that would result in virtually no deflection.

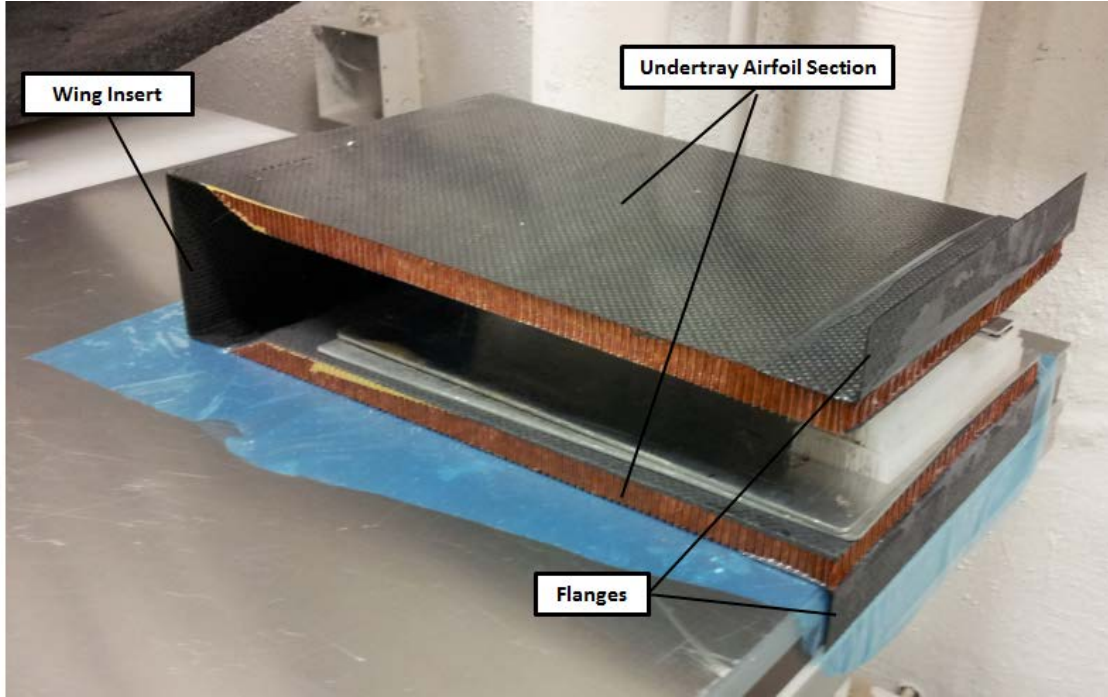


Figure 24: Undertray test sample

The structure was fastened to a plate and loaded with about 130 N (the estimated amount of downforce per side at 65 KPH from CFD). If the CFD simulation was accurate, each side of the undertray would theoretically produce 443 N at the maximum speed of 120 KPH (since downforce increases by the square of the velocity). However, designing for this worst case scenario that will likely never happen (based on the poor performance of past undertrays) would add a lot of weight. Therefore, it was reasonable to only load this test sample up to 130 N. Even then though, the undertray test sample deflected too much. No measurements were taken, but it was clear that these flanges needed more strength.

#### 5.3.1.4. c-Car Flange Layup Schedule

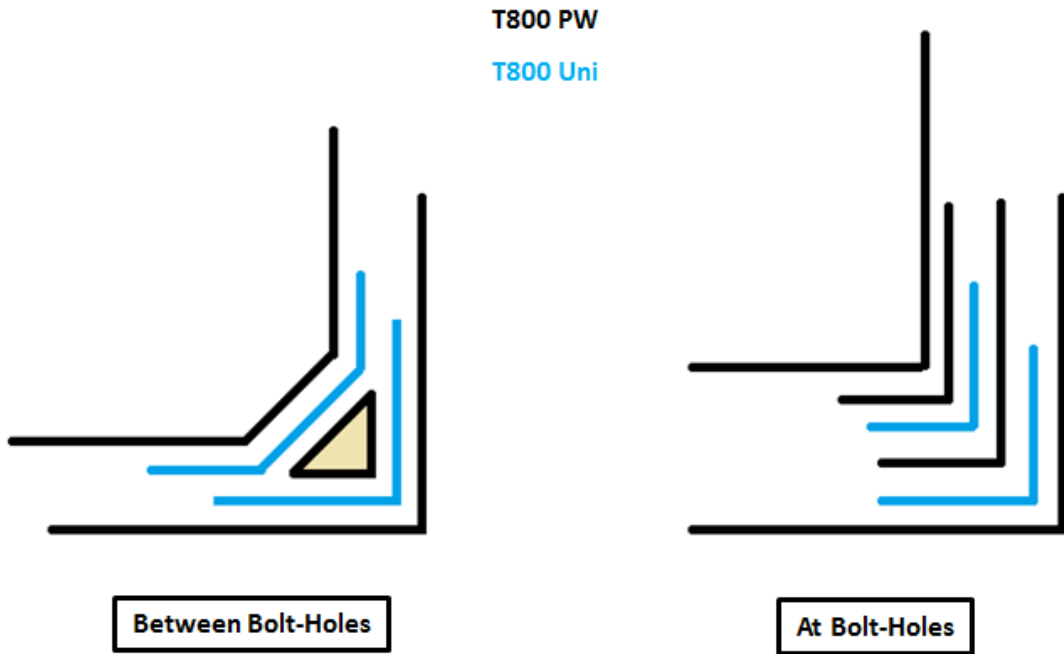


Figure 25: Layup schedule used for c-Car flanges

Due to the success of using core to increase stiffness in other parts, the layup schedule shown in *Figure 25* was proposed that uses a core gusset between layers of T800 PW and layers of T800 Uni in the corner. It was hoped that the addition of the core would produce the necessary stiffness without adding too much weight. At the bolt-hole locations, the core stops to leave room for washers. Two extra layers of T800 PW will be laid up at these bolt-hole locations to reduce the chance of the fasteners shearing out. Plain weave carbon fiber was chosen over unidirectional carbon fiber to reinforce the fastening points because preventing shear-out failures require strength in more than one direction.

#### 5.3.1.5. e-Car Flange Layup Schedule

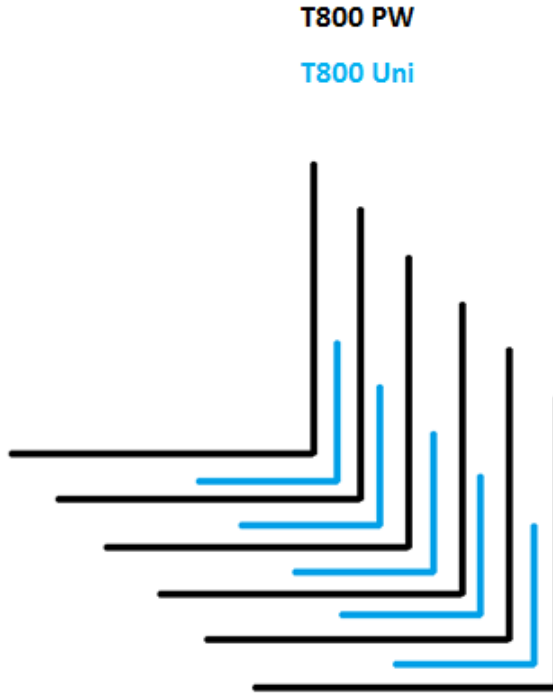
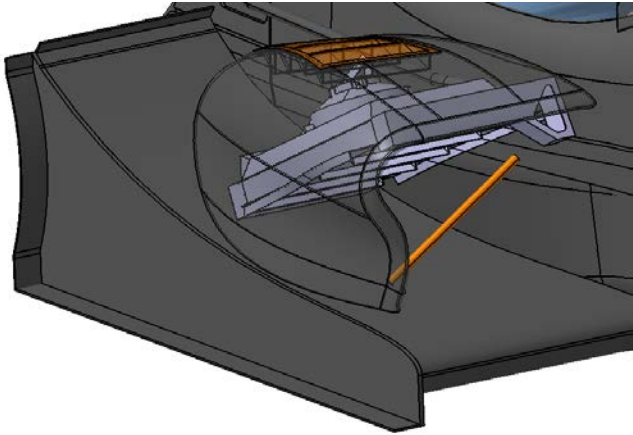


Figure 26: Layup schedule used for e-Car flanges

Without the side-pods on the e-car, there would be nothing to hide the drop link. Therefore, to see if the flanges could be strong enough to support the undertray without the added support from the drop link, the flanges for the e-car will be over built with 11 total layers in the corner (6 layers of T800 PW and 5 layers of T800 Uni alternating), as shown in *Figure 26*. This should be more than enough to support the downforce produced by the undertray, but there is still a chance a strong cone impact could damage it. The e-Car will only compete at European competitions though, which use much smaller cones than at Formula SAE Michigan.

### 5.3.2. Drop Link



*Figure 27: Undertray drop link inside side-pod*

The location of the drop link was chosen so that it could be as long as possible, but still stay within the side-pod of the c-Car and leave enough room for the radiator. The drop link will be 0.5-inch diameter aluminum tube stock with plastic rod-ends on each side to connect to clevises on the chassis and undertray. The clevises will be connected to the undertray and chassis with M4 potted inserts.

## 5.4. Splitter Structure and Integration

The structure of the splitter depended on how it was going to be integrated. The goal was to come up with a design where the splitter would have all its degrees of freedom constrained, but not interfere with the bottom-out post in the case of a bottom-out. To accomplish this, the splitter flat plate will have two sheet metal brackets epoxied in the front for mounting to the front sway bar bolts, and two sheet metal brackets epoxied in the back for mounting to the seat belt mount. Using these existing mounting

locations, which can be seen in , eliminates the need to change the chassis any further. Also the sheet metal brackets will provide sufficient rigidity, but will buckle out of the way in the case of a bottom-out. As for the splitter panels, it will be divided into two straight sections and two curved sections. These panels will be fastened to L-brackets on the flat plate with plastic rivets, which will allow for easy removal of the panels if necessary.

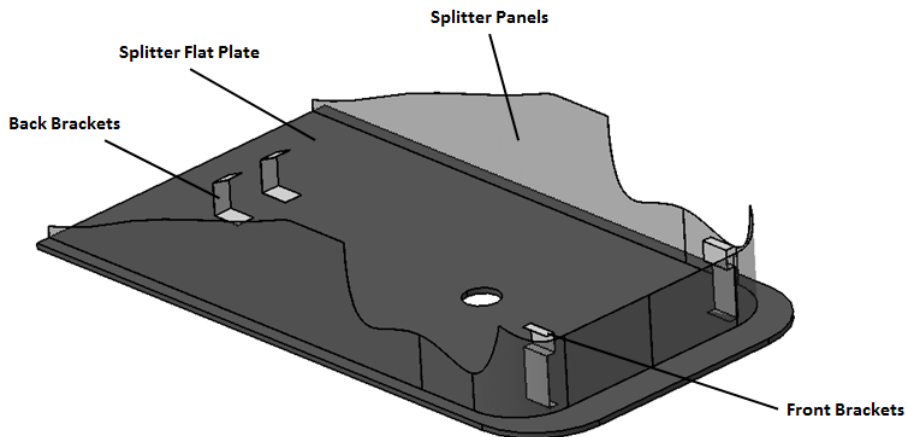


*Figure 28: Undertray splitter with mounting brackets*

#### **5.4.1. Splitter Flat Plate**

The splitter flat plate will be flush with the bottom of the chassis. Therefore, it will be 32 mm (static ride height of chassis) above the ground. There is a hole in it for the bottom-out post.

##### *5.4.1.1. Splitter Flat Plate Layup Schedule*

Like the rest of the undertray, the splitter flat plate will be made using a “1-core-1” layup schedule for sufficient rigidity and to keep it lightweight. For added abrasion

resistance, a layer of Kevlar will be added along the edges and along the front since these are the locations most likely to hit the ground. This layup schedule is shown in *Figure 29*.

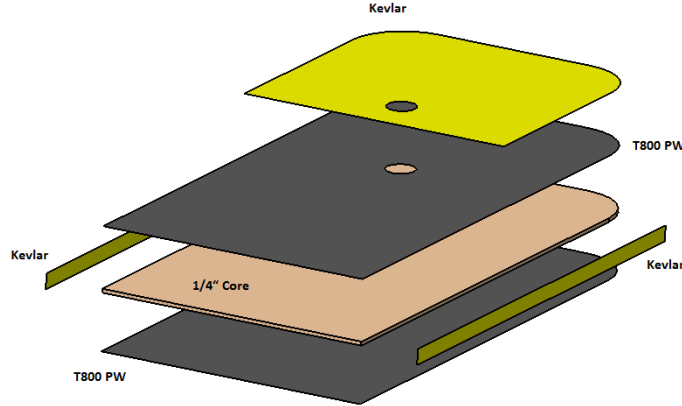


*Figure 29: Layup schedule for splitter flat-plate*

#### **5.4.2. Splitter Panels Layup Schedule**

The splitter panels are responsible for covering up the underbody of the vehicle to reduce the drag induced by the suspension assembly as much as possible.

##### *5.4.2.1. Splitter Panels Layup Schedule*

In order to squeeze in between the undertray and chassis, the panels will need to be rather flimsy. Therefore, it will only be 2 plies of T800 PW. The edge that butts up against the chassis will need to be covered with edge tape to prevent scratch marks.

#### **5.4.3. Brackets**

The front bracket is shaped the way it is to not interfere with the front sway bar and allow room for a wrench to tighten the bolt onto the nut. They will be made out of aluminum 1/16" thick aluminum sheet metal. The back brackets on the other hand will be

made from 1/16" thick steel sheet metal so that a steel nut can be welded to it. The bracket needs to have a nut with threads because it would be very difficult to reach both sides of the seat belt mount to tighten a fastener onto a nut.

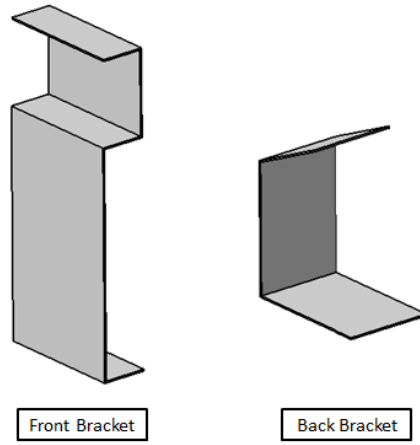


*Figure 30: Splitter mounting brackets*

## 5.5. Mechanical Design Summary

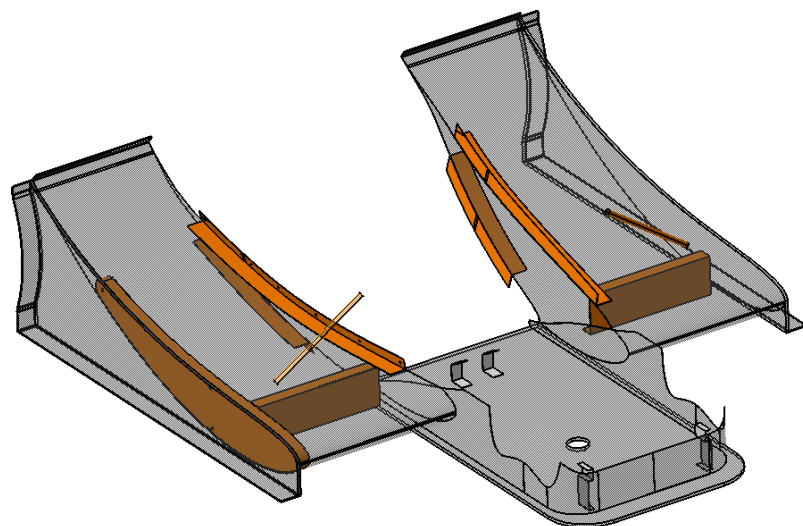


*Figure 31: Mechanical design of undertray*

The mechanical design of the undertray, as shown in *Figure 31*, is the result of reasoned engineering thought. While not many calculations or FEA simulations were done to support this concept, not dwelling on the theory allows for these parts to actually be manufactured to determine whether it is actually sufficient or not.

In order to get a rough estimate of the final mass of the undertray, the area of the four largest parts (airfoil section, wing insert, endplate, and splitter flat plate) was measured in CAD and multiplied by the weight per area of carbon fiber and core test sample pieces. The results are shown in *Table 5*. This could be an overestimate since it was assumed core was everywhere, but could also be an underestimate since other parts were not considered and paint (clear coat) was not considered. Nonetheless, a reasonable goal is to have the whole undertray under 4 kg, or 8.8 pounds.

<i>Table 5: Undertray Mass Estimate</i>					
Part	Area [m <sup>2</sup> ]	Plies	Core	Parts	Mass [g]
Undertray Airfoil	0.71	2	1	2	1879
Undertray Endplate	0.41	2	1	2	1085
Wing Insert	0.12	2	0	2	161
Splitter Flat	0.58	2	1	1	767
<b>Total</b>					<b>3892 g</b>

## 6. MANUFACTURING DESIGN

Manufacturing this undertray will require a number of tooling to be developed. Section 6 details the thought behind the design of these tools.

### 6.1. Materials Available

*Table 6* lists the materials that were available through sponsorship or from a supplier to make the molds for the undertray.

<i>Table 6: Mold Materials Available</i>	
Material	Data Sheet
RenShape 5008	[15]
Ren-Weld 5008	[16]
Medium Density Fiberboard (MDF), $\frac{1}{2}$ " thick	N/A

RenShape 5008 is an epoxy board material designed for prepreg layup tools that can go up to  $250^\circ$  [15]. The boards can be bonded together and repaired with Ren-Weld 5008 adhesive, which has the exact same properties. RenShape has very good machinability, results in a good surface finish, and is cheaper and lighter than aluminum, making it the most preferable material for carbon fiber tools. It is still fairly expensive and in limited supply however, making medium density fiberboard a reasonable alternative. It is more difficult to machine and work with, but it can result in parts that are just as good.

### 6.2. Undertray Mold (Airfoil Section)

Like the rear and front wings, the undertray airfoil section will be made in two halves from female molds by dividing the airfoil at the extremum at the leading edge and

at the extremum at the trailing edge. A simple top and bottom female mold as shown in *Figure 32* was the first design iteration. While these molds would be simple to manufacture, it will be very difficult to match the contour of the chassis if it is not built into the mold. Therefore, walls were built into the mold that matched the exact contour of the chassis. The height of the walls was sized at 0.55-inches so that the  $\frac{1}{2}$ -inch core could butt up against it. While this mold is more complex, it will save a significant amount of time down the road when fitting the part to the vehicle, and will likely look a lot better. This final design iteration of the undertray mold is shown in *Figure 33*. Areas for clamping in the CNC were added to the mold. These molds will be made from REN Shape 5008 and machined using a 3-axis CNC machine. Making these large molds using a CNC, instead of by hand out of MDF like past undertray molds, will save a significant amount of time.

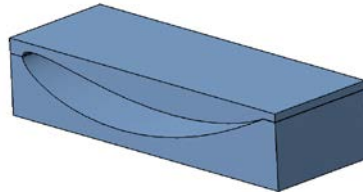


*Figure 32: Undertray mold initial design iteration*

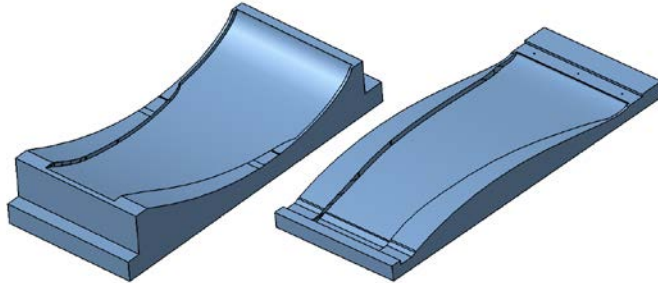


*Figure 33: Undertray mold final design iteration*

To create the joggle on the top half of the undertray, the mold shown in *Figure 34* was conceived. A close-up of the joggle offset can be seen in Figure 35. The joggle mold will be connected to the top halve mold with 3 M4 bolts. To clamp this part in the CNC and make the G-code generation easier, the joggle mold was remodeled to look like *Figure 36*.

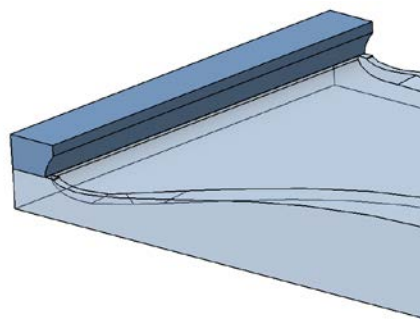


*Figure 34: Undertray joggle mold on the top half mold*

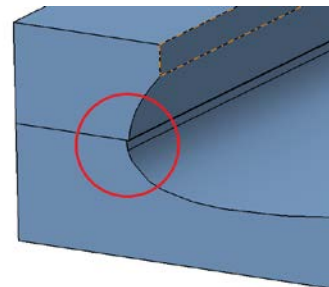


*Figure 35: Close-up of undertray joggle mold on the top half mold*

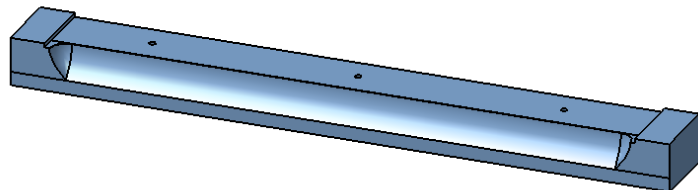


*Figure 36: Joggle mold remodeled to generate G-code easier*

### 6.3. Undertray Wing Insert Mold

The first design concept of the wing insert mold is shown in *Figure 37*. It is the same exact contour of the airfoil, except offset inward by 0.020-inches, the estimated thickness of 2-ply of carbon fiber plus the bond gap. The mold is split laterally for easy removal of the part once it cures.

Using REN Shape 5008 for all molds would be optimal since the cheaper option, MDF, is much harder to machine and seal. For simple 2D parts like this wing insert mold though, using MDF is much more practical since REN Shape 5008 is expensive and the supply is limited. Therefore, MDF was chosen as the material for the wing insert mold. Since MDF should not be machined inside a closed CNC machine (because the organic powder will get into the coolant and possibly grow mold), the wing insert mold was broken up even further into 4 different parts so that it would fit an open CNC mill. This final design iteration is shown in *Figure 38*. Each of these parts needs to be machined on only 2 sides, leaving the other 2 sides for clamps. The parts that go together have a “puzzle piece” where epoxy will be applied to connect them. The two halves of the wing insert mold will then be fastened to an aluminum plate to be held in place for carbon fiber layup.

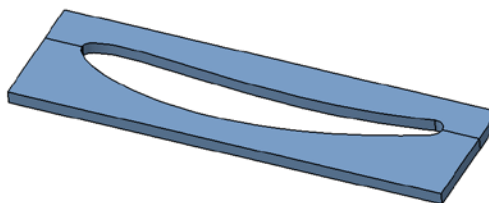


*Figure 37: Wing Insert Mold first design concept*

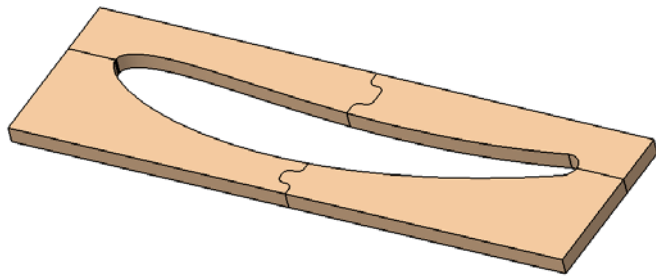


*Figure 38: Wing Insert Mold final design concept*

#### **6.4. Undertray Endplate Mold**

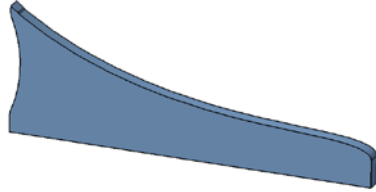


*Figure 39: Undertray endplate mold first design concept*

While endplates have always been laid up on flat plates in previous years, they did not have any side-skirts. Seeing as the undertray endplate has an outer side skirt and a tire deflector, a mold was conceived that would allow these additions to the endplate to be laid up with the endplate as opposed to bonded on afterward. The first design iteration is shown in *Figure 39*.

Like the wing insert mold though, this is a simple 2D part that will not need the benefits of REN Shape 5008. Therefore, MDF was chosen as the mold material for the undertray endplate mold as well. While cutting the undertray endplate mold by hand with a jigsaw like the front and rear endplate molds was considered, using a CNC was selected

instead to make sure the contour of the airfoil on the endplate would be exact. Like the wing insert mold, this required the part to be broken up into smaller pieces to fit on the Bridgeport. The segmented part is shown in *Figure 40*. The mold also has the 4 bolt-hole locations that are machined using the CNC as well. These will be used to accurately locate the location of the weld nuts on the wing insert.

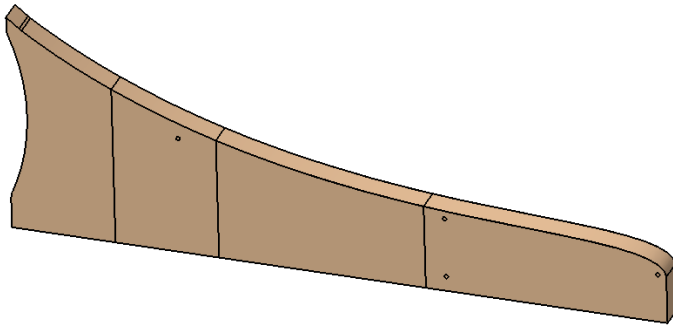


*Figure 40: Undertray endplate mold final design concept*

It is important to note that unlike the undertray wing insert mold, the individual parts of the undertray endplate mold will not be connected by puzzle pieces and are instead flat and will be connected by dowels pins. This is because unlike the wing insert mold, each of these individual parts needs to be machined on all 4 sides. To mount a part whose entire perimeter is being CNC profiled, regular vices or clamps cannot be used because it would interfere with the end-mill. To solve this problem, typically holes are drilled into it so that a fastener can clamp through it. The surface of the undertray endplate however is the mold surface and cannot be drilled into. Therefore, to machine all 4 sides and keep it fastened down, 2 sides of the part can be profiled first while the other 2 sides are held down. Once that is finished, the recently machined sides can be fastened

down and the mounts on the 2 un-machined sides can be taken off, allowing the CNC to machine the remaining 2 sides. If the part were to move however in this transfer of clamps, the location of the CPL that the CNC machine uses as a reference has moved. Therefore, it was decided to keep all interface sides flat just in case they needed to be used as a reference for the CNC machine. The location of the dowel pins that will connect these parts will be located by hand using precision measuring tools.

## 6.5. Undertray Top Flange Mold

In order to create a flange that would match the contour of the undertray and the chassis, the mold shown in *Figure 41* was conceived.

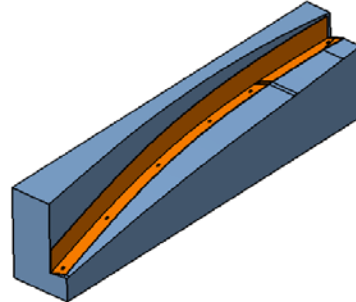


*Figure 41: Top Flange Mold initial design concept*

This mold would be impossible to create in a CNC however, due to the sharp corner that is less than 90 degrees. Therefore, the mold was broken up into two parts, one that matched the undertray contour and one that matched the chassis contour. This final design concept is shown in *Figure 42*. The chassis-side top flange mold will have the contours of both sides, while only one of the undertray-side top flange molds will be manufactured. Therefore, two different oven cures will be required to make both sides.

Also in the final design iteration are the six bolt-hole locations. Since this is a complex part that requires high accuracy to replicate the chassis and undertray surfaces, this mold will be manufactured out of REN Shape 5008 for the good machinability.

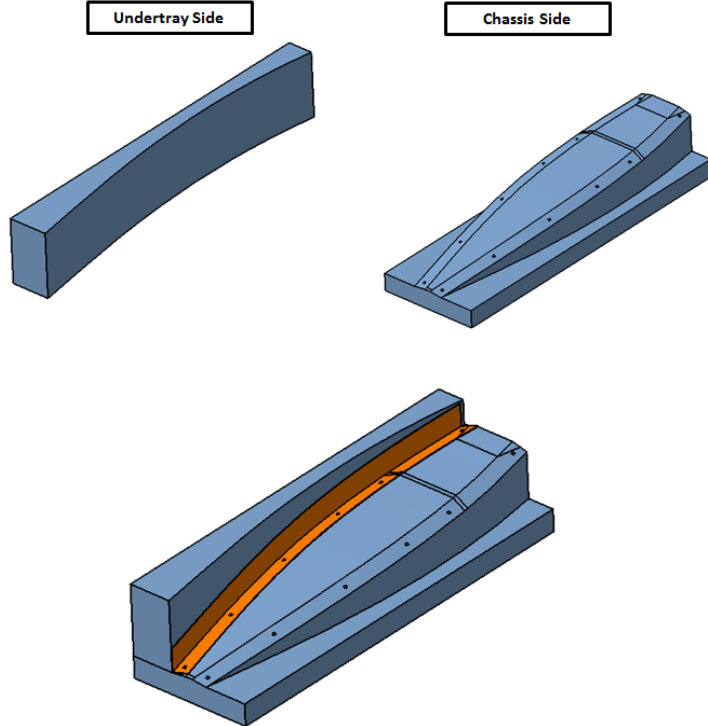


*Figure 42: Undertray Top Flange Mold final design concept*

## 6.6. Undertray Bottom Flange Mold

To create the bottom flange, the mold shown in Figure 41 was conceived that will allow the flanges for both sides to be made at the same time. The bottom flange is more than 90 degrees, making that sharp corner manufacturable by a CNC. Excess material that might interfere with the CNC tool was removed and four bolt-hole locations were added, along with a section for clamping in the CNC for the final design iteration shown

in *Figure 44*. Like the top flange mold, this mold will be manufactured out of REN Shape 5008.

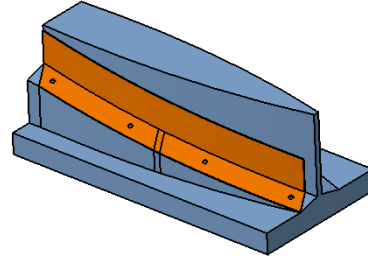


*Figure 43: Bottom flange mold initial design concept*

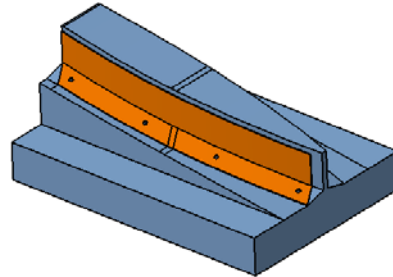


*Figure 44: Bottom flange mold final design concept*

## 6.7. Remaining Molds and Tools

All other parts of the undertray, including the gurney flap, spar, and splitter, will not need any new tools. In other words, they will be laid up on aluminum or MDF bar stock or sheet metal.

## 6.8. Manufacturing Design Summary

While past GFR undertrays have been made with hand shaped MDF molds, all 7 of the molds described in this section will be made on a CNC. This will much faster, and

will enable the production of two undertrays in one season for the first time in GFR's history.

*Table 7* lists all the parts for the undertray, per car. Since GFR will be manufacturing two cars, the actual amount of parts is double what is shown (except for the tooling parts). All parts will be manufactured in-house, unless specified otherwise.

<i>Table 7: Undertray Parts List</i>			
<b>Part</b>	<b>Part Number</b>	<b>Quantity</b>	<b>Description</b>
<b>Tooling</b>			
Top Mold	--	1	REN Shape 5008, CNC
Bottom Mold	--	1	REN Shape 5008, CNC
Joggle Mold	--	1	REN Shape 5008, CNC
Top Flange Mold	--	2	REN Shape 5008, CNC
Bottom Flange Mold	--	1	REN Shape 5008, CNC
Endplate Mold	--	4	MDF, CNC Bridgeport
Wing Insert Mold	--	4	MDF, CNC Bridgeport
<b>Carbon Fiber</b>			
Airfoil Top (Right)	GFR_13_10_42_100_11	1	1-core-1 with uni in trailing edge
Airfoil Bottom (Right)	GFR_13_10_42_100_12	1	1-core-1 with uni in trailing edge
Spar (Right)	GFR_13_10_42_100_13	1	1-core-1
Wing Insert (Right)	GFR_13_10_42_100_14	1	2 plies of T800 PW
Endplate (Right)	GFR_13_10_42_100_15	1	1-core-1 with 5 layers in skirt
Top Flange (Right)	GFR_13_10_42_100_16	2	2-core-2 with reinforcement at bolts
Bottom Flange (Right)	GFR_13_10_42_100_17	2	2-core-2 with reinforcement at bolts
Airfoil Top (Left)	GFR_13_10_42_100_21	1	1-core-1 with uni in trailing edge
Airfoil Bottom (Left)	GFR_13_10_42_100_22	1	1-core-1 with uni in trailing edge
Spar (Left)	GFR_13_10_42_100_23	1	1-core-1
Wing Insert (Left)	GFR_13_10_42_100_24	1	2 plies of T800 PW
Endplate (Left)	GFR_13_10_42_100_25	1	1-core-1 with 5 layers in skirt
Top Flange (Left)	GFR_13_10_42_100_26	2	2-core-2 with reinforcement at bolts
Bottom Flange (Left)	GFR_13_10_42_100_27	2	2-core-2 with reinforcement at bolts
Gurney Flap	GFR_13_10_42_100_31		5 plies of T800 PW

Splitter Flat Plate	GFR_13_10_42_100_41	1	1-core-1 with Kevlar reinforcement
Splitter Panels	GFR_13_10_42_100_42	4	2 plies of T800 PW
<b>Other Parts</b>			
Drop Link	--	2	1/4" aluminum tube
Plastic Rod Ends	--	4	Ordered from igus ®
M6 Fasteners	--	8	Ordered from supplier
M4 Fasteners	--	26	Ordered from supplier
M6 Washers	--	8	Ordered from supplier
M4 Washers	--	26	Ordered from supplier
M6 Weld Nuts	--	8	Ordered from McMaster-Carr
M4 Potted Insert	--	18	Aluminum, CNC lathe
M6 Flanged Potted Insert			
Front Splitter Brackets	--	2	Aluminum 1/16-inch sheet metal
Back Splitter Brackets	--	2	Steel 1/16-inch sheet metal
M4 Nut	--	2	Ordered from supplier
1/16" Thick SBR Rubber	--	2	Ordered from supplier

## 7. MANUFACTURING

Section 7 will detail the manufacturing process for the undertray, from the fabrication of the molds to the integration to the vehicle.

### 7.1. Tooling Parts

The following sections will go into brief detail of the manufacturing of the tooling parts from *Table 7*.

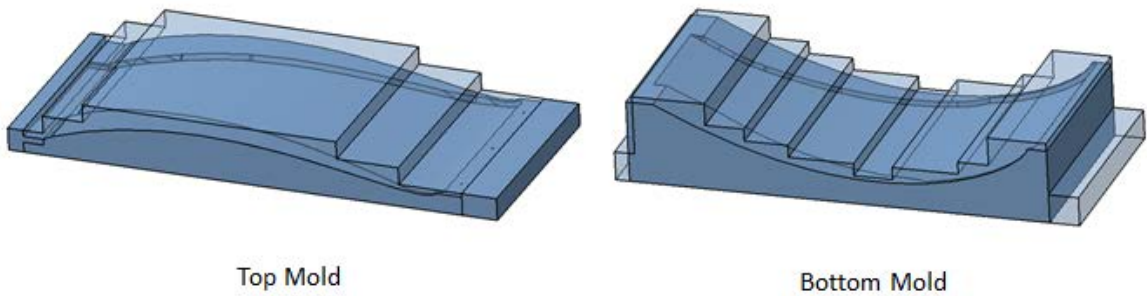
#### 7.1.1. Undertray Airfoil Section Molds

##### 7.1.1.1. Making the Stock for the Undertray Airfoil Section Molds

Making the stock for undertray airfoil section molds started with looking at the available boards of RenShape 5008 from the available supply. Using the thickness of the boards available, the stock was sized in CAD with a minimum offset of 0.5 inches, as shown in *Figure 45*. The stocks for the undertray airfoil section molds were then made using the following process, as shown in *Figure 46*:

1. Cut the RenShape boards to specified dimensions using a circular or table saw.
2. Glue the boards together with Ren-Weld.
3. Clamp the mold securely for a 24 hour cure cycle.

With a gel time of only 75 minutes, the bonding of the different stocks had to be done in multiple sessions to allow for enough time to place the boards on top of each other accurately.



Top Mold

Bottom Mold

Figure 45: Stock for top and bottom mold sized in CAD



Figure 46: Making the stock for the undertray airfoil section molds

#### 7.1.1.2. CNC Machining the Undertray Airfoil Section Molds

The G-code was generated by exporting the solid models as STL files and importing them into Edge-CAM. All geometry was selected manually in Edge-CAM to make sure the part was divided into the appropriate regions. The recommended roughing speed and feed rate were 1600 RPM speed and 40 IPM feed for a 1 in. 4-flute end mill, while the recommended finishing speed and feed were 10,000 RPM speed and 100 IPM feed for a 5/8 in. 2-flute ball end mill [15]. These parameters were used to calculate the appropriate feeds and speeds for roughing and finishing for the tools available in the machine shop using the following equations:

$$\text{Spindle RPM} = \frac{\left(\text{Recommended Speed } \left[\frac{\text{ft}}{\text{min}}\right]\right) * 12}{\pi * (\text{Tool Diameter})}$$
$$\text{Feed} = 0.001 \times \left(\text{Recommended Feed } \left[\frac{0.001 \text{ in}}{\text{tooth}}\right]\right) (\text{Flutes})(\text{Spindle RPM})$$

Each part had a roughing code, a finishing code, and if necessary, a code to drill holes. The roughing pass took off most of the material with a 0.030" offset, and the finishing pass came in to give a smooth surface finish with a 0.002" cusp height. Each of the large molds took more than 5 hours of machining. An illustration of the tool paths generated from Edge-CAM can be seen in *Figure 47*.

To machine REN Shape, the CNC machine needed to be thoroughly cleaned and covered in plastic to ensure the blue RenShape dust would not get into the coolant system, as shown in *Figure 48*. The stocks were then put into a Fadal 4525, fastened down, and machined as shown in *Figure 49*.

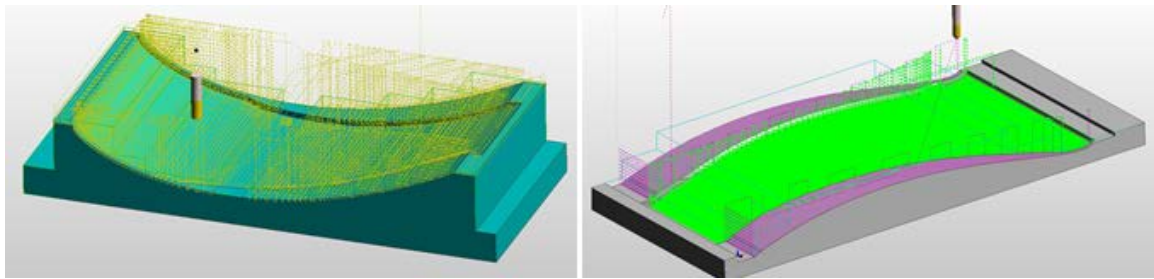


Figure 47: Roughing and finishing passes for undertray molds



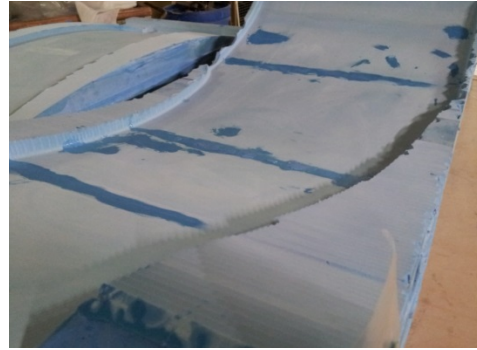
Figure 48: Cleaning and covering the CNC machine



Figure 49: Machining the joggle and top half undertray mold

#### *7.1.1.3. Finishing the Undertray Airfoil Section Molds*

Once the molds were machined, they were then sanded, filled and repaired with Ren-Weld (as shown in *Figure 50*), sanded again, sealed with REN Shape Performance Sealer, and then wet sanded. The finished molds can be seen in *Figure 51*.



*Figure 50: Filling in gaps in the mold with REN-Weld*



*Figure 51: The finished and sealed undertray molds*

#### **7.1.2. Undertray Wing Insert Mold**

##### *7.1.2.1. Making the Stock for the Wing Insert Mold*

To make the stocks for the wing insert molds, the following process was followed (as shown in *Figure 52*):

1. Cut out  $\frac{1}{2}$ " thick MDF boards to the appropriate dimensions from CAD
2. Glue the boards together with generic wood glue to make a 1" thick MDF board
3. Clamp together for overnight curing



*Figure 52: Making the stock for the wing insert molds*

#### 7.1.2.2. CNC Machining the Wing Insert Mold

All the wing insert molds for the front wing, rear wing, and undertray were machined the same way. The G-code was fairly simple for these parts, since it only involved 2-dimensional profiling. Instead of chipping away at the part, only the contour

of the wing insert mold would be cut and the excess material would just fall off, as shown in *Figure 53*. Without documentation on machining MDF, different feeds and speeds were tested, as shown in *Figure 54*. Ultimately, what worked the best was a high speed of 3000 RPM with 30 IPM feed for a 3/8" 2-flute end mill (both roughing and finishing). The finish from these parameters can be seen in *Figure 55*. These parts were done on the Bridgeport CNC mill, as opposed to the Fadal CNC machine, so that the MDF powder would not get into the coolant.

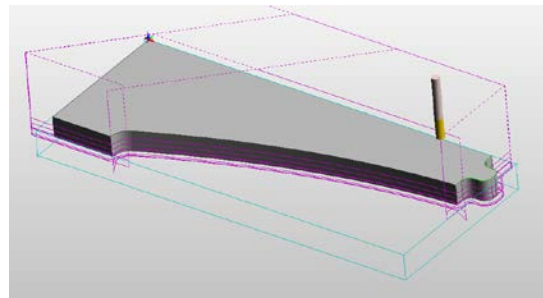


*Figure 53: Profiling tool path for one of the undertray wing insert parts*



*Figure 54: Dialing in the right feeds and speeds for machining MDF*



*Figure 55: Wing insert molds after being machined*

#### *7.1.2.3. Finishing the Wing Insert Mold*

The puzzle piece used to connect the pieces of the undertray wing insert mold was successful, as shown in *Figure 56*. The molds were then sealed with all-purpose fiberglass resin, as shown in *Figure 57*. A better option would have been to use Duratec Polyester Surfacing Primer to seal the molds, but fiberglass resin worked on previous test samples and was the more cost effective solution. An aluminum plate was then cut for each of the wing insert molds so that they had something to bolt to. The finished undertray wing insert mold is shown in *Figure 58*.



*Figure 56: Undertray wing insert puzzle piece connection*



*Figure 57: Sealing wing insert molds*



*Figure 58: Finished undertray wing insert mold*

### **7.1.3. Undertray Endplate Mold**

#### *7.1.3.1. Making the Stock for the Undertray Endplate Mold*

The MDF stock was made using the same procedure for the stocks for the wing insert, except the undertray endplate used three  $\frac{1}{2}$ " thick boards instead so that a 30 mm skirt could be made.

#### 7.1.3.2. CNC Machining the Undertray Endplate Mold

The machining of the undertray endplate mold pieces used the exact same parameters from the wing insert mold parts. However, as explained in 6.4, only two sides of each piece were machined at time (as shown in *Figure 59*) so that the entire perimeter could be profiled while keeping the part clamped. This turned out to be a good idea, since a machining mistake did occur, as shown in *Figure 60*. The piece was put back onto the Bridgeport CNC, and the straight edges were used as a reference to CNC machine the part again.

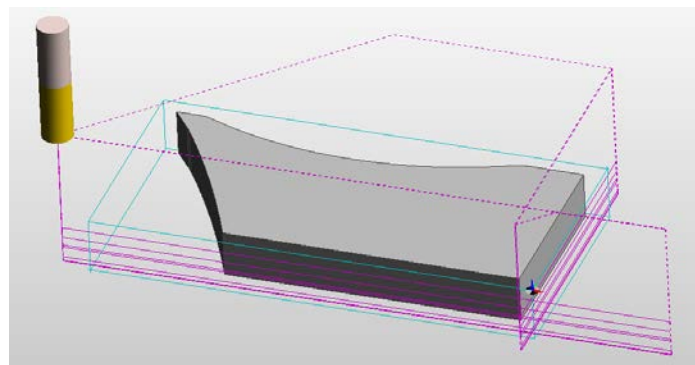


*Figure 59: Profiling tool path for the undertray endplate mold back piece*



*Figure 60: Undertray endplate mold machining mistake*

#### *7.1.3.3. Finishing the Undertray Endplate Mold*

The individual pieces of the endplate were connected together with dowel pins and then glued together with all-purpose fiberglass resin (wood glue was not used due to the larger bond gap required). The endplate was then sanded to create a smooth surface. Initially, the fiberglass resin was going to be used to seal the mold like the wing insert mold. However, as shown in the test sample in *Figure 62*, the veneer of the MDF board came right off. Therefore, the mold will be covered either in mold tape, or release film and peel ply to seal the mold.



*Figure 61: Undertray endplate mold after being glued and sanded*



*Figure 62: Failed attempt at sealing the surface of the MDF board*

### 7.1.4. Undertray Flange Molds

#### 7.1.4.1. Making the Stock for the Undertray Flange Molds

Making the stock for the flange molds followed the same procedure as making the stock for the undertray airfoil section molds.

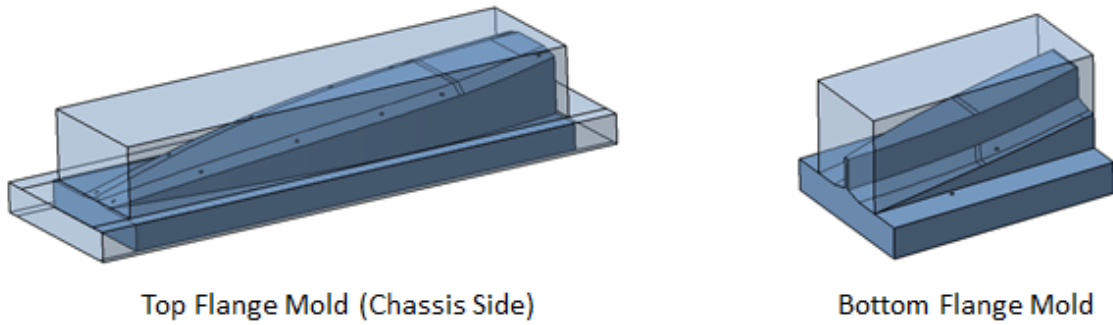


Figure 63: The stock for the top flange mold sized in CAD

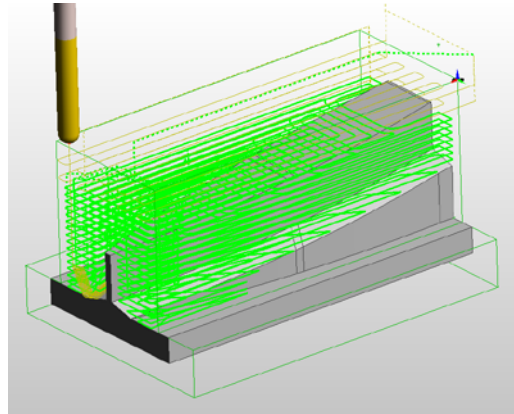


Figure 64: Making the stock for the flange molds

#### 7.1.4.2. CNC Machining the Undertray Flange Molds

The CNC machining of these molds followed the same procedure as the machining of the undertray airfoil section molds. However, while all finishing passes have been calculated in Edge-CAM using the “parallel lace” algorithm, the bottom flange

mold was the exception. Since the mold surface changed in the X, Y, and Z direction, a parallel lace would have caused the tool to run into the mold. Therefore, boundaries were carefully selected and the “project flow curves” algorithm was used instead to move the tool in the X, Y, and Z direction simultaneously, as shown in *Figure 65*.



*Figure 65: Tool path for the finishing pass of the bottom flange mold*



*Figure 66: Machining the top flange molds*

#### 7.1.4.3. Finishing the Undertray Flange Molds

The flange molds were finished using the same procedure as the undertray airfoil section molds. For the top flange mold, holes were drilled into the side so that an

aluminum block could be fastened to it and hold the two pieces in place, as shown in *Figure 67*.



*Figure 67: Finished undertray top flange mold together*



*Figure 68: Finished undertray bottom flange mold*

## 7.2. Carbon Fiber Parts

The following sections will briefly detail the carbon fiber layup process for each of the parts of the undertray.

### 7.2.1. Oven Cures

Since the RenShape molds are very brittle, the datasheet recommended a cure cycle up to 250°F starting at room temperature with an hour hold at every 50°F [16]. To eliminate the need to come in and hold the oven every hour, a constant slow ramp rate of 25 degrees per hour was chosen to allow time for the molds to reach the oven temperature. Once at 250°F, testing has shown that T800 needs approximately 10 hours to cure. Afterwards, the oven would ramp down at the same rate of 25 degrees per hour. If there were no RenShape molds in the oven (i.e. only MDF molds), then a ramp rate of 60 degrees per hour was selected.

### 7.2.2. Undertray Airfoil Sections

#### 7.2.2.1. *Templates for Undertray Airfoil Section*

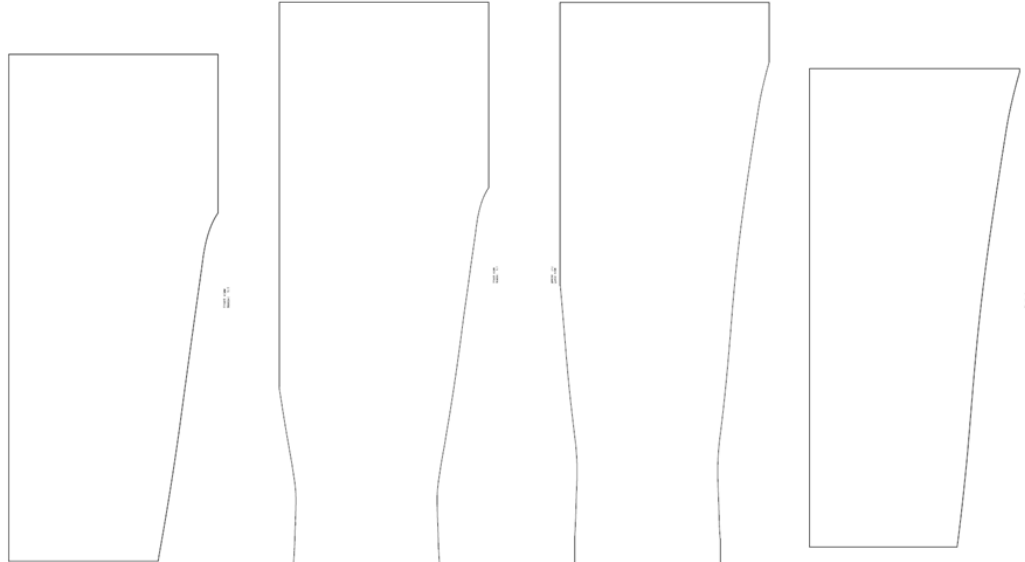
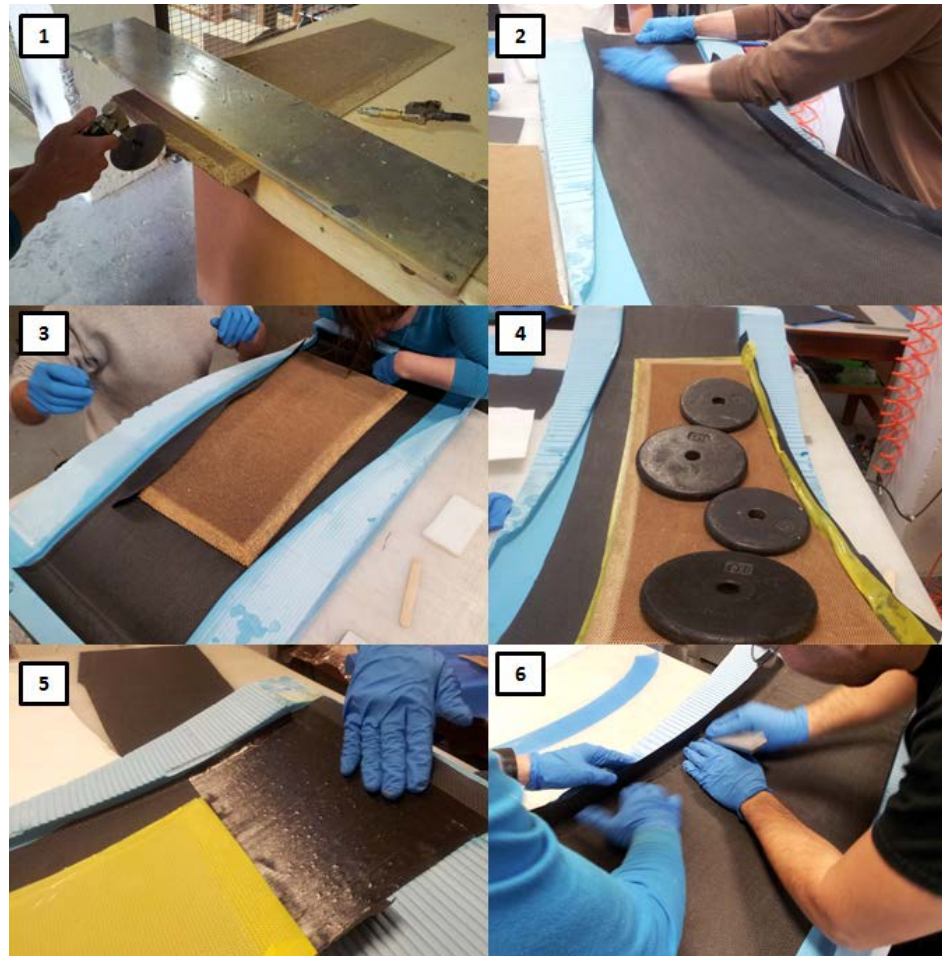


Figure 69: Undertray carbon fiber and core templates

To make the layup easier, carbon fiber and core templates were created in CAD, as shown in *Figure 69*. The carbon fiber is over-estimated to account for errors, and will need to be cut off once cured.

#### 7.2.2.2. Layup of the Undertray Airfoil Sections



*Figure 70: Layup of the undertray airfoil section*

With the templates and the chassis contour built into the mold, the layup was rather straight forward. The following general procedure was used (as shown in *Figure 70*, *Figure 71*, and *Figure 72*):

1. Cut and taper core to prevent bridging in the sandwich structure.
2. Lay the first layer of carbon fiber down.
3. Lay the core piece down.
4. Shape the core to the shape of the mold with weights and a heat gun.
5. Apply uni to the trailing edge.
6. Cover all exposed core to prevent it from acting like a sponge in the rain and increasing in weight.
7. Create the joggle on the undertray top half airfoil section by cutting off excess material with the joggle mold off, putting the joggle mold on, and then laying carbon fiber into the joggle.
8. Vacuum bag the part making sure it is not overly stretched in any pockets.



*Figure 71: Creating the joggle on the top half undertray airfoil section*



*Figure 72: Vacuum bagging the undertray bottom mold*



*Figure 73: Both sides of the undertray airfoil section*



*Figure 74: Wing halves connected at the leading edge with the joggle*

### 7.2.3. Undertray Wing Inserts

#### 7.2.3.1. Templates for the Undertray Wing Insert

Since the wing inserts are only 2 plies of carbon fiber with no core, the layup process was fairly simple. To create the layer that matched the shape of the wing insert, the backing of the carbon fiber was cut to make a template, as shown in *Figure 75*.



*Figure 75: Carbon fiber backing used as a template*

#### *7.2.3.2. Layup of the Undertray Wing Inserts*

With no core, the layup process was fairly simple. The most difficult part of laying up the wing inserts was making sure there was no bridging in between layers at the corners. When vacuum bagging, it was important that the release film and peel ply were not bridging either. All the finished wing inserts for one aero package can be seen in *Figure 77.*



*Figure 76: Front wing insert being laid up*



*Figure 77: All the wing inserts for one aerodynamics package*

## 7.2.4. Undertray Endplate

### 7.2.4.1. Making the Hard-points for the Undertray Endplate



Figure 78: T800 PW 1/4-inch hard-point plate

To create the  $\frac{1}{4}$ " thick hard-points for reinforcement at the bolts inside the endplate, a plate containing 26 layers of T800PW was laid up. A layup schedule of 26 layers was chosen because the chassis team used 52 layers of T800 PW to create their  $\frac{1}{2}$ " hard-point plate. The plate ended up being slightly less than  $\frac{1}{4}$ " since the thickness does not increase linearly with plies, but this ensured that it would not be thicker than the core.

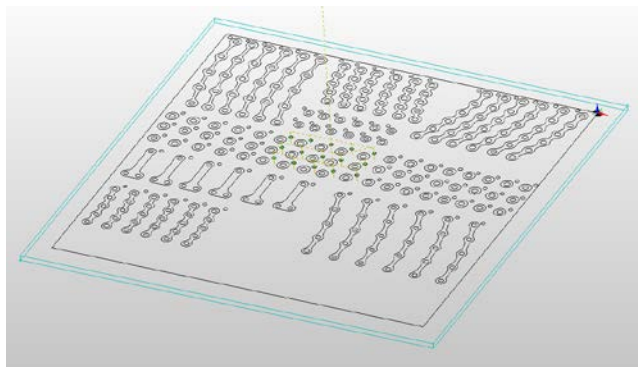


Figure 79: The hard-point plate inside Edge-CAM

The bolt-holes were then drilled into the plate, along with the starter holes for the water jet on a CNC machine. The G-code for drilling the holes had to be broken up every

15 holes so that the drill bit could be replaced. The plate was then taken to the water-jet sponsor to be cut-out.



*Figure 80: Water-jetting the hard-point plate*



*Figure 81: Finished hard points*

#### 7.2.4.2. Layup of the Undertray Endplate

The following process was used to layup the undertray endplate (as shown in *Figure 82*):

1. Use endplate mold to cut core into endplate shape; place on mold to cut holes for the hard-points at the bolt-hole locations.
2. Seal the mold either with mold tape, or release film and peel ply.
3. Lay down the continuous skirt layer.

4. Lay down the first global undertray layer.
5. Drape the global layer over the tire deflector by cutting relief strips.
6. Layup the layers supporting the skirt and tire deflector.
7. Laydown the glue sheet and core.
8. Laydown the last global undertray layer.

A finished and sealed undertray endplate can be seen in *Figure 83*.

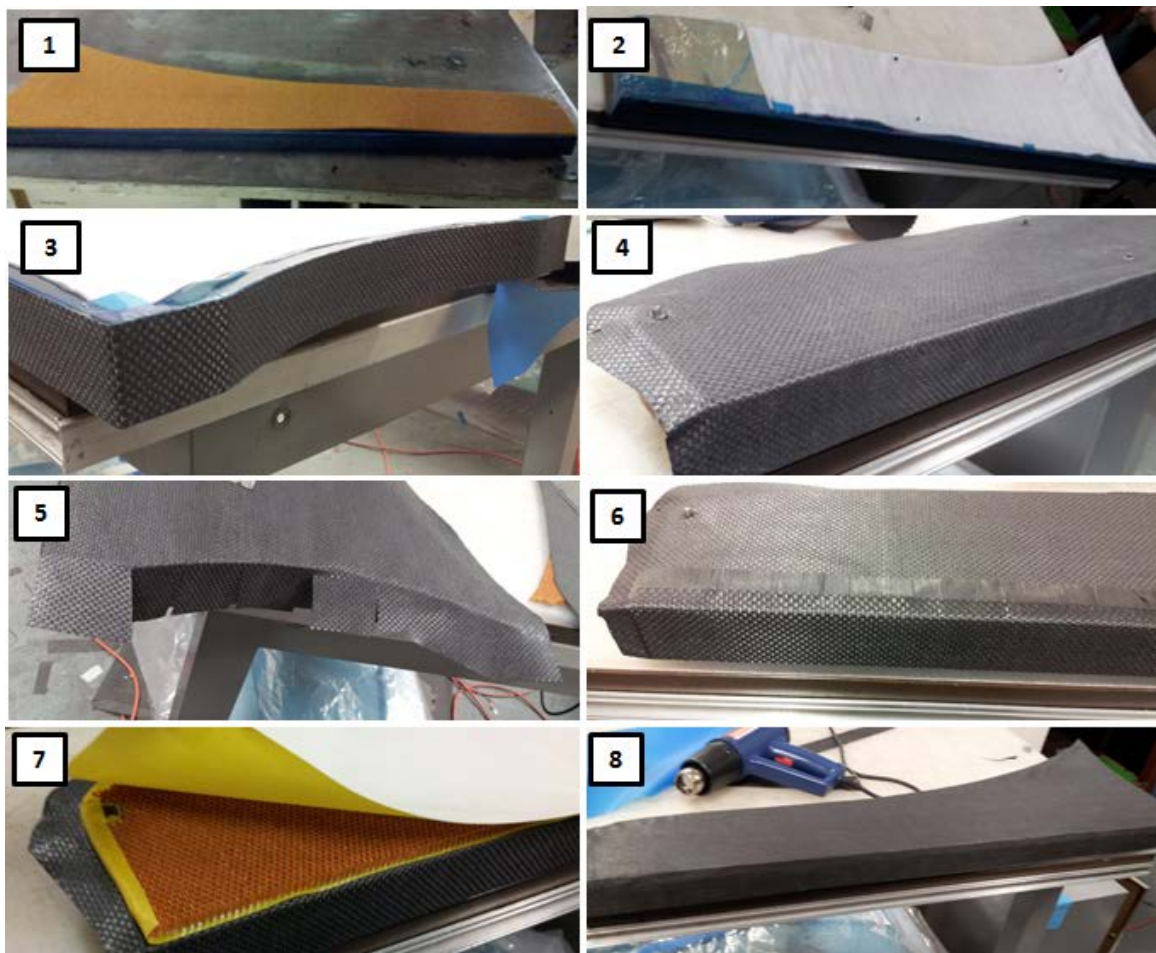


*Figure 82: Using the undertray endplate mold to cut the core*



*Figure 83: Finished and sealed undertray endplate*

#### 7.2.5. Undertray Flanges

The process to create the c-Car flanges with the core gussets is shown *Figure 84*.

The holes for the bolts were on the mold. So, after each layer was laid down, a sharp tool was used to poke the hole through (after curing, the holes were drilled out). A trick to apply the glue sheet for the core was to wrap the core gussets in the glue sheet before laying it down. They were fairly difficult to make and were prone to bridging. Regardless, they turned out well and were strong, as shown in *Figure 85*.



*Figure 84: Layup of the c-Car undertray top flanges (with core gussets)*



*Figure 85: Finished c-Car undertray flanges*

For the e-Car, flanges were made without core, making them significantly simpler and easier to make, as shown in *Figure 86*



*Figure 86: Layup of the e-Car undertray top flanges (no core)*

### 7.2.6. Spars and Gurney Flaps

The spars were simply “1-core-1” and the gurney flaps were just a 5-ply thick. For molds, MDF stock pieces were cut to the right dimensions and sealed with either mold tape or wrapped in release film and peel ply, as shown in *Figure 87*.



*Figure 87: MDF spar and gurney flap molds*

### 7.2.7. Undertray Splitter

#### 7.2.7.1. Template for the Splitter Flat Plate

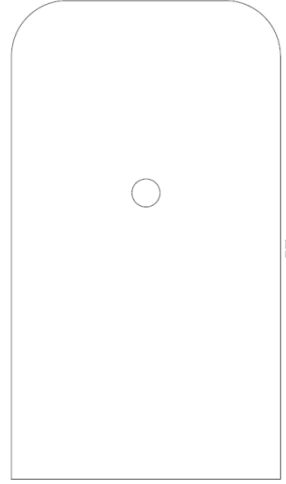


*Figure 88: Splitter flat plate template*

To create the splitter, the template shown in *Figure 88* was used to cut the core and the carbon fiber pieces.

#### 7.2.7.2. Layup of the Splitter Flat Plate

The layup process of the splitter flat plate was very easy, as shown in *Figure 82*. However, since it was so large, it was important to pick a flat plate that was large enough that it could be laid up and also vacuum bagged. It was also important to make sure all edges, including the edges of the hole for the bottom-out post, had at least two layers to make sure no core would be exposed and soak up rain water.



*Figure 89: Splitter flat plate layup process*



*Figure 90: Bottom of cured splitter flat plate*

#### 7.2.7.1. Layup of the Splitter Panels

The flat sections the splitter panel was laid up on the flat plate with the slitter flat plate, the curved sections were laid up on the curved aluminum sheet metal shown in *Figure 91*. The cured panel sections can be seen in *Figure 92*.



*Figure 91: Curved aluminum sheet metal used as molds for the curved panels*



*Figure 92: Cured panels of the splitter*

## 7.3. Finishing

The following section will cover the finishing process of the undertray, including trimming and bonding. *Figure 93* shows the preliminary fitting of all the parts of the undertray.



*Figure 93: Side-view of preliminary assembly of the undertray*

### 7.3.1. Trimming

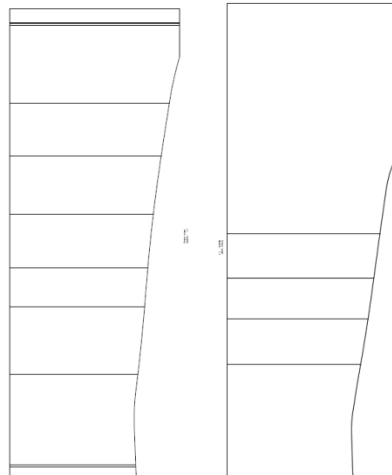


*Figure 94: Undertray trimming templates*

To make sure the edge that went up against the endplate was straight, the templates shown in *Figure 94* was used. Along with having the straight edge, these

templates also have the locations of the bolt-holes for the flanges. The process in using these templates were the following (images of these steps are shown in *Figure 95*):

1. Line the template with the straight edge on the leading edge, drape it back, and tape it down.
2. Use masking tape to mark the straight edge.
3. Remove the template to reveal the straight edge.
4. Tape the other side of the straight edge. This is done so that the straight edge reference is visible during cutting, as opposed to being cut off.
5. Remove the original piece of masking tape to reveal the straight edge.

Once an air grinder removed most of the excess material, the edge was then sanded down to the tape, as shown in *Figure 96*.

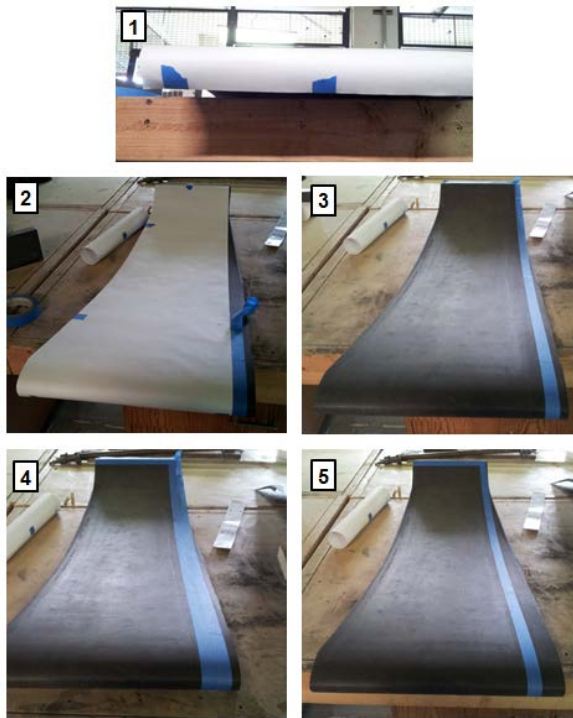


*Figure 95: Process used to get straight edge for cutting*

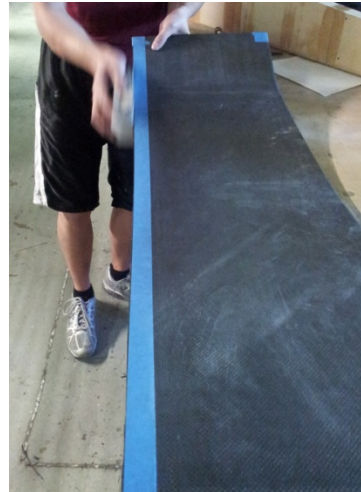


*Figure 96: Sanding down to the masking tape*

### **7.3.2. Bonding**

Hysol 9380 [13] was used for most of the bonding. After some failed bonds, Hysol 9340 [14] was used instead.

#### *7.3.2.1. Weld Nuts to Wing Insert*

To bond the weld nuts to the wing insert, the endplate was used as a reference, as shown in *Figure 97*. Some of the weld-nuts needed to be grinded down to go up against the edge of the wing insert.



*Figure 97: Weld-nuts located using endplate*

### 7.3.2.2. Undertray Airfoil, Spar, and Wing Insert

The bonding of the undertray airfoil section assembly was done in two sessions, as shown in *Figure 98*:

1. Leading edge
2. Trailing edge, wing insert, and spar

It was also important to mask off parts of the undertray that should not get any epoxy prior to bonding. After carefully applying the epoxy, the parts were held in place with a variety of clamps. To prevent epoxy from getting on the clamps, release film was used. The parts were put in the oven at 180 degrees for one hour, as recommended by the data sheet [14]. Once cured, the parts were taken out and sanded down.

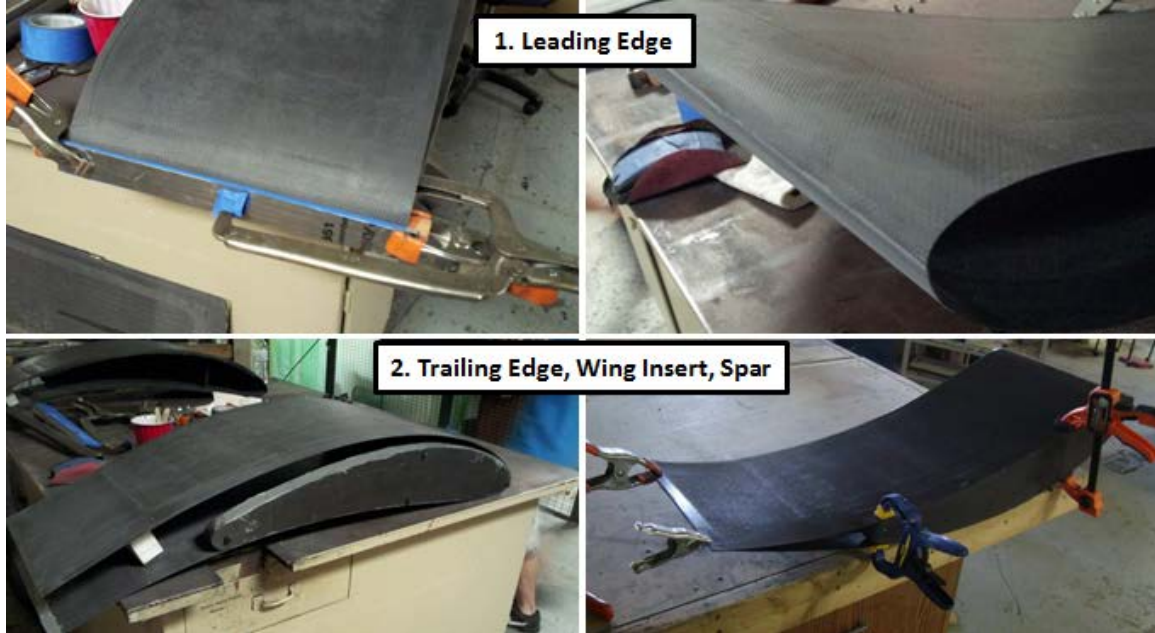


*Figure 98: Bonding the Undertray Airfoil, Spar, and Wing Insert*

## 7.4. Undertray Airfoil Section Integration

### 7.4.1. Locating on the Chassis

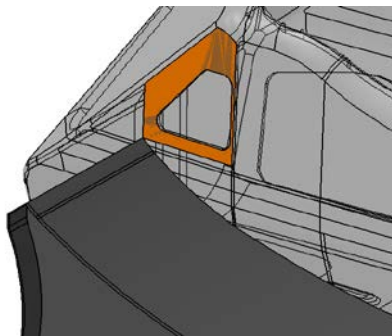


*Figure 99: Undertray Locator Template*

To locate the undertray onto the chassis, the following process was used (as shown in *Figure 100*):

1. Place the chassis on to a precision table. Set the angle of the undertray by fastening it to the endplate, and placing the skirt of the endplate on the table surface. Elevate the skirt to 21.27 mm (dimension from CAD) off the table in the Z direction. The Z dimension is now constrained.
2. Set the X location by using the template shown in *Figure 99* to locate the trailing edge. Also set the Y location by pushing the undertray against the chassis. Since the contour of the chassis was built into the mold, it should fit the first time.
3. Support the inside of the undertray, and an inclinometer was used to make sure it is level.
4. Set the flanges down at the approximate locations using the templates from *Figure 94*, and find where it fits best. Mark the location of the flange on the

undertray and the location of the bolt holes on the chassis. The undertray is now ready to be taken off the chassis for bonding.

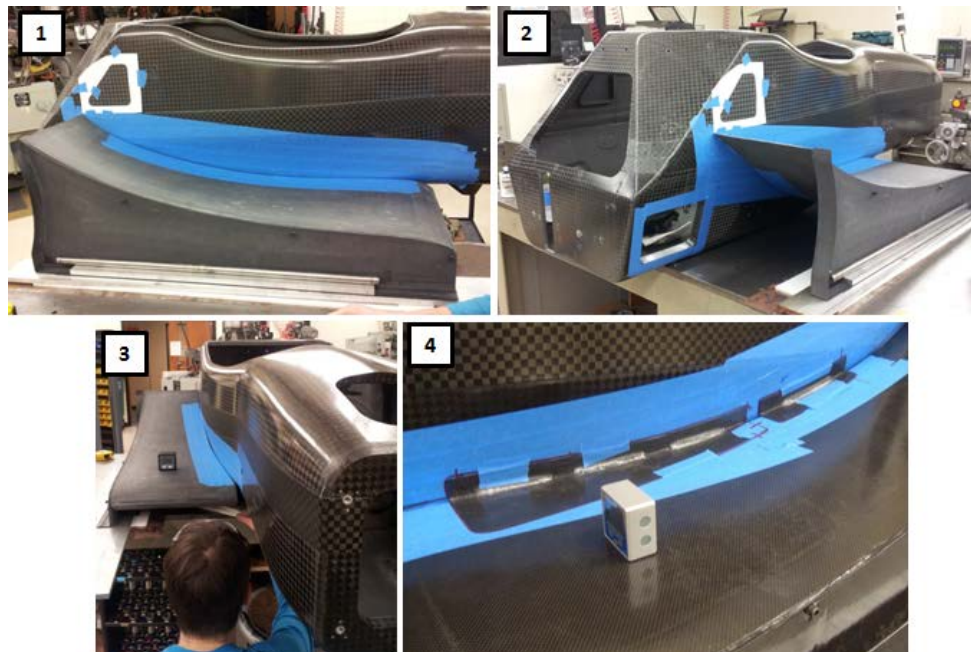


*Figure 100: Marking the location of the flanges*

*Figure 101* shows the flange being clamped in place to the undertray with clekos during bonding. After this was finished, the airfoil section of the undertray was complete. Windows were cut out of the wing insert to reduce weight further.

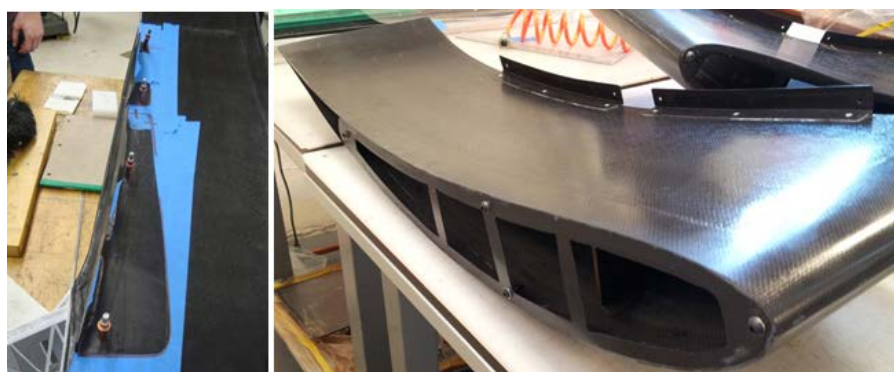


*Figure 101: Bonding the flanges to the undertray*

The bolt-hole locations on the chassis were drilled out, and inserted with epoxy for the potted inserts, as shown in *Figure 102*. The chassis before and after can the potted inserts were glued into the chassis can be seen in *Figure 103*.



*Figure 102: Gluing potted inserts into the chassis for the undertray*



*Figure 103: Before and after the potted inserts were glued in*

#### 7.4.2. Mounting the Undertray Airfoil Section to the Chassis

With the bonding complete, the undertray was then mounted to the chassis, as shown in *Figure 104*.



*Figure 104: Side-view of undertray on chassis*

### 7.4.3. Finishing Touches

The last few touches for the undertray include the addition of the gurney flap and the drop link. The gurney flap was taped on (as shown in *Figure 105*), as opposed to glue on to allow for on-off testing. The drop link on the other hand, required more drilling and the insertion of a potted insert into the chassis and the undertray, as shown in *Figure 106* and *Figure 107*.



*Figure 105: Gurney flap taped to undertray*



*Figure 106: Drop links for the undertray*



*Figure 107: Drop link on the undertray and chassis*

## 7.5. Undertray Splitter Section Integration

### 7.5.1. Splitter Flat Plate Integration

The sheet metal brackets were made by simply cutting and bending sheet metal to the right dimensions. The front brackets had two holes drilled into each of them so that they could be fastened to the front sway bar bolts. The back brackets had an M4 nut welded to it so an M4 bolt could be fastened to it through the seat belt mount.

Once these brackets were mounted to their respective locations underneath the chassis, the splitter flat plate was held up to the underside of the vehicle, and the locations of the brackets were marked on masking tape. The brackets were then taken off and epoxied to the flat plate at those marked locations. While this method was not the most accurate method, the sheet metal brackets were not completely rigid, which allowed some room for error. Also epoxied to the flat plate were the L-brackets the splitter panels will be fastened to with plastic rivets. The finished flat plate can be seen in *Figure 108*.



*Figure 108: Brackets epoxied to splitter flat plate*

### 7.5.1. Splitter Panel Integration

The splitter panels were cut to the approximate shape using the template shown in *Figure 109*. They were then sanded down to fit on the car, and attached to the splitter flat plate with plastic rivets that went into carbon fiber L-brackets on the flat plate. When integrated to the chassis, Velcro was added to keep the panels on.

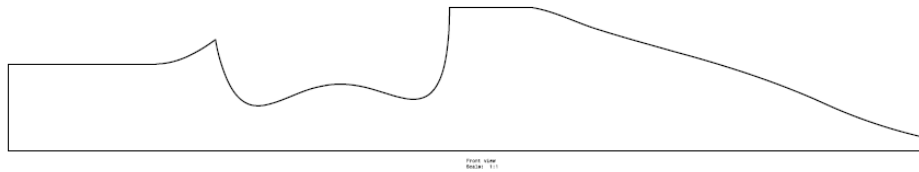


*Figure 109: Splitter panel template*

### 7.5.1. Mounting the Splitter to the Chassis

*Figure 110* shows the splitter mounted to the chassis. It required two people to mount: one to hold the splitter up to the bottom of the chassis, and one to screw in the fastener to the back bracket.



*Figure 110: Finished splitter with panels*

## **7.6. Manufacturing Summary**

It took 21 weeks to completely manufacture and integrate the first aerodynamics package for the combustion vehicle (front wing, rear wing, undertray, and side-pods), and an additional 4 weeks to finish the second aerodynamics package (front wing, rear wing, and undertray). The following lists the total parts that were made in-house this year for both aerodynamics packages, including those that had to be re-made:

- 6 RenShape Mold Parts
- 26 MDF Mold Parts
- 202 Carbon Fiber Parts

## **8. TESTING**

Section 8 will detail the testing performed thus far to validate the undertray design. Due to short time constraints, driver training was the highest priority and not many well-controlled aerodynamic and mechanical tests were performed.

### **8.1. Aerodynamic Testing**

#### **8.1.1. On-Off Testing**

To see the immediate effect of the aerodynamics package, the vehicle was run with wings on and wings off. Since removing the undertray with the side-pods and radiators in the way took some time, it was decided to run the vehicle with the undertray still on the vehicle during the “off” phase. With the wings, lap times were reduced by 6.63 percent. While this is a promising result for the wings, this test did not provide any indication of the performance of the undertray.

#### **8.1.2. Coast-Down Testing**

To get an approximate measurement of downforce, coast down tests were performed. This is when the vehicle accelerates and then coasts in neutral with the clutch engaged so that no power is transferred to the wheels. As a result, the vehicle decelerates from the aerodynamic drag and the springs of the suspension are compressed by the aerodynamic downforce. The amount of downforce can then be extrapolated from the level of compression of the springs.

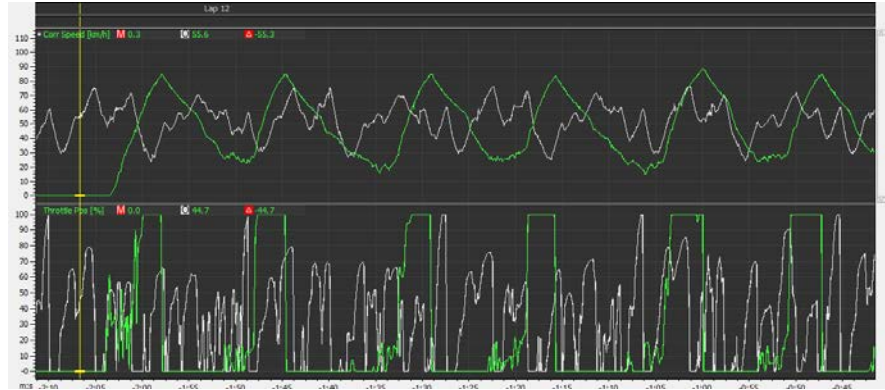


*Figure 111: Car speed data during coast-down testing*

After a series of coast-down tests (as shown in *Figure 111*), the data indicated that the vehicle was producing about 867N of downforce at 65 KPH. If it is assumed that CFD was completely accurate for the wings, the coast down data suggests that the undertray is making some level of downforce to help get the whole vehicle up to 867N.

### 8.1.3. Pressure Tapping

To measure the pressure gradient underneath one side of the undertray, an 8-x-4 grid of pressure taps were installed on the right undertray, as shown in *Figure 112*. Another pressure tap was installed on the roll hoop to measure the static pressure of free stream air, as shown in *Figure 113*. All these pressure taps were connected to the differential pressure sensor underneath the vehicle to measure the difference in pressure between the free stream air and the air underneath the undertray.



Figure 112: Pressure taps connected to the differential pressure sensor



Figure 113: Static pressure tap and Pitot tube on top of the roll hoop

#### 8.1.3.1. Raw Data

The raw data of the pressure tapping data correlated rather well, as shown in Figure 114. In other words, as air speed increased (measured by the Pitot tube), the differential pressure between the underside of the undertray and free stream also increased as expected.

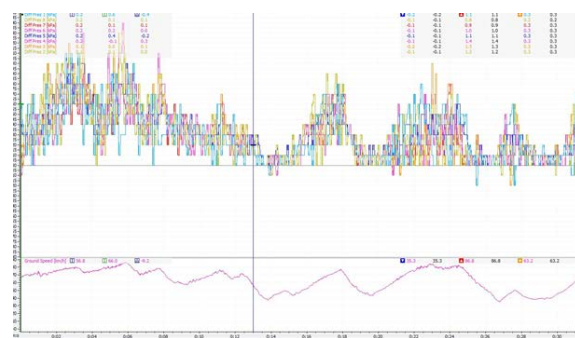


Figure 114: Differential pressure and speed raw data

### 8.1.3.2. Pressure Gradient Results

With only 8 channels on the differential pressure sensor, getting data from all 32 pressure taps required 4 different runs. The best way to do this would be to record pressure from a straight line drive at constant speed. However, as stated before, driver testing was the most important and pressure tapping data was secondary. Therefore, pressure tapping was recorded on the following 4 runs instead:

- (1) **Row 1:** May 3; Driver - Ryan Thoma; Asymmetric Oval 1
- (2) **Row 2:** May 4; Driver - Robert Story/Jenson Vliss; Skid-pad
- (3) **Row 3:** May 3; Driver - Ryan Thoma; Autocross 1
- (4) **Row 4:** May 4; Driver - Phillip Arscott; Endurance 4

The data was then filtered by speed, averaged, and then fitted to a 3D grid in MATLAB.

The pressure gradient from CFD for comparison is shown in *Figure 115*.

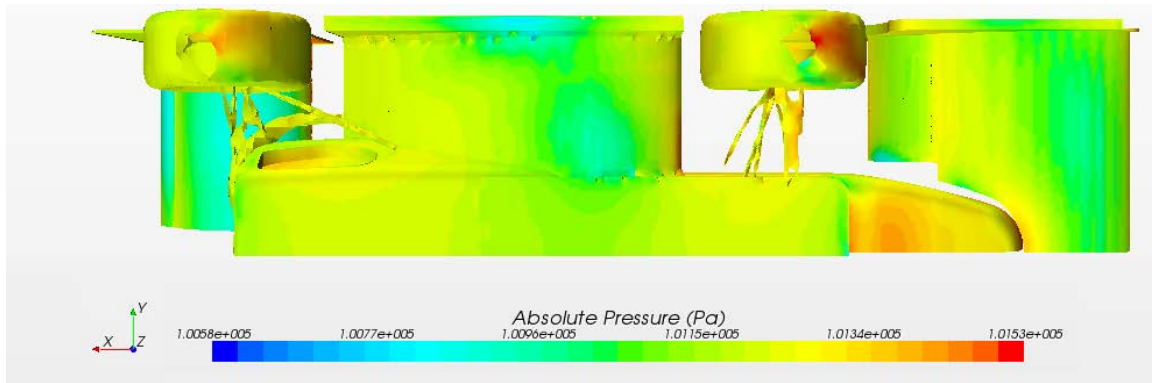


*Figure 115: Undertray pressure gradient from CFD*

*Figure 116* and *Figure 117* depict the pressure gradient for 45 KPH. The lowest pressure region is actually on the outside of the undertray. Since these data points were recorded during non-straight track runs, the car was mostly likely turning at 45 KPH.

Therefore, this data may be indicating that this was where the air was fastest. The average differential pressure over the region is 0.19 kPa.

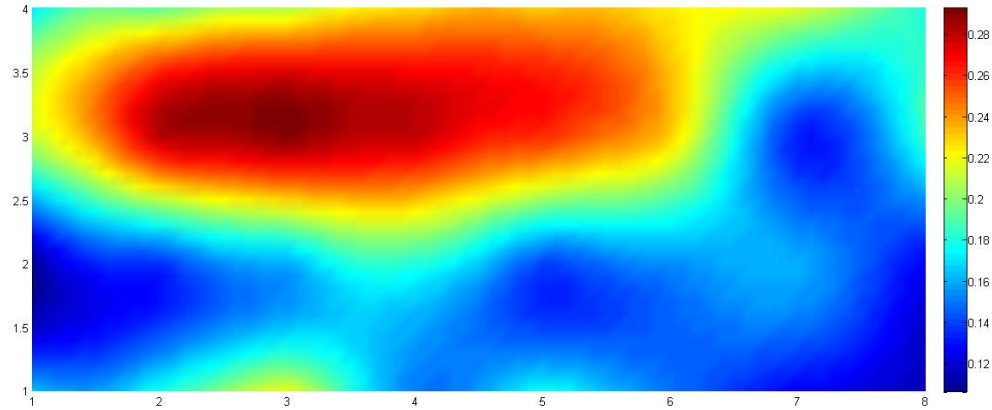


Figure 116: Pressure gradient for 45 KPH

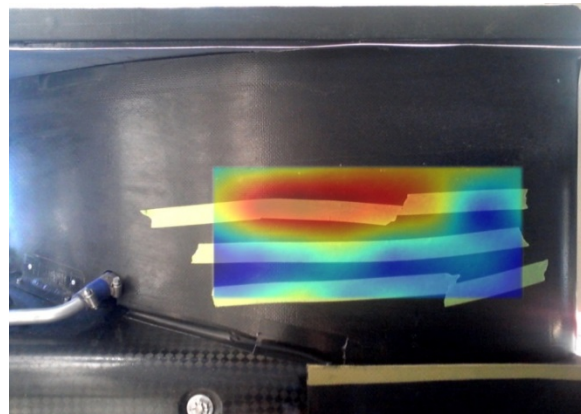


Figure 117: Pressure gradient for 45 KPH with undertray

Figure 118 and Figure 119 depict the pressure gradient for 65 KPH, the usual average speed for an FSAE course. Since Row 2 was recorded during a skid-pad run, no data points at 65 KPH existed. Therefore, it was omitted from the results.

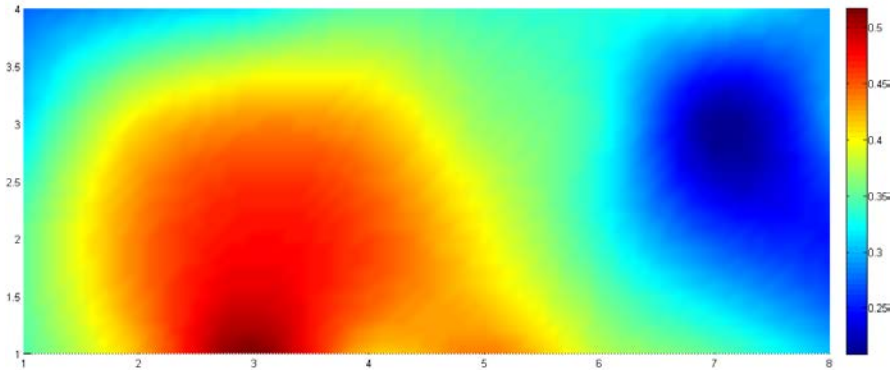


Figure 118: Pressure gradient for 65 KPH



Figure 119: Pressure gradient for 65 KPH with undertray

Figure 120 and Figure 121 depict the pressure gradient for 80 KPH. Like the 65 KPH data, Row 2 was omitted. The average pressure is 0.52 kPa.

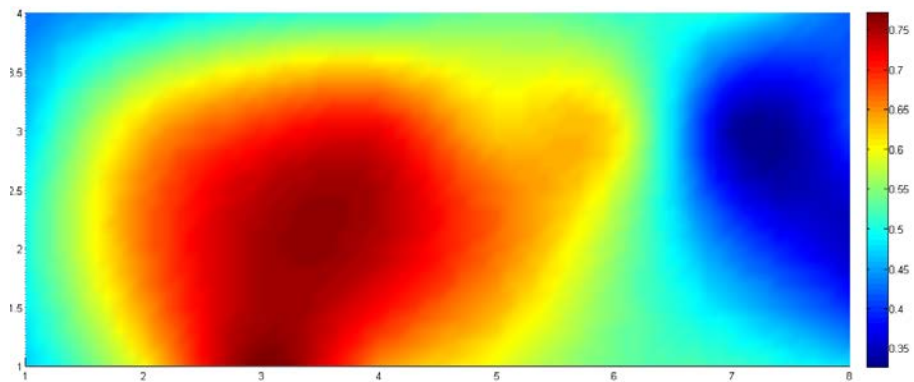


Figure 120: Pressure gradient for 80 KPH



*Figure 121: Pressure gradient for 80 KPH with undertray*

### **8.1.1. Aerodynamic Testing Summary**

There is definitive proof that aerodynamics plays a large role in overall Formula SAE vehicle performance, and that the wings make a significant fraction of the downforce. What is not clear is the exact contribution of the undertray. Given more time, better designed experiments should be implemented with proper calibration and randomization. Possible further tests include improved pressure tapping with higher resolution data, strain gauging the front and rear wing, pressure tapping the front and rear wing, on-off testing of the undertray (particularly on the e-car with no side-pods), flow visualization, and wing tunnel testing.

## **8.2. Mechanical Testing**

### **8.2.1. Actual Mass**

Each part of the undertray was weighed after being sealed. The results can be seen in *Table 8*. The total weight of the undertray was about 3.9 kg (8.6 pounds), not including fasteners and the drop link. This measurement matched extremely well with the estimate from *Table 5*, and is less than half the weight of the 2011 undertray.

*Table 8: Actual Undertray Mass*

<b>Part</b>	<b>Part Number</b>	<b>Mass [g]</b>
Airfoil Top (Right)	GFR_13_10_42_100_11	470
Airfoil Bottom (Right)	GFR_13_10_42_100_12	480
Spar (Right)	GFR_13_10_42_100_13	37
Wing Insert (Right)	GFR_13_10_42_100_14	96
Endplate (Right)	GFR_13_10_42_100_15	400
Top Flange (Right)	GFR_13_10_42_100_16	50
Bottom Flange (Right)	GFR_13_10_42_100_17	28
Airfoil Top (Left)	GFR_13_10_42_100_21	470
Airfoil Bottom (Left)	GFR_13_10_42_100_22	480
Spar (Left)	GFR_13_10_42_100_23	37
Wing Insert (Left)	GFR_13_10_42_100_24	96
Endplate (Left)	GFR_13_10_42_100_25	400
Top Flange (Left)	GFR_13_10_42_100_26	50
Bottom Flange (Left)	GFR_13_10_42_100_27	28
Splitter Flat Plate	GFR_13_10_42_100_31	682
Splitter Panels	GFR_13_10_42_100_32	85
<b>Total</b>		<b>3889 g</b>

### 8.2.2. Mechanical Failures

After 5 weeks of driving the vehicle, the undertray held up very well mechanically. However, some components did break, particularly the outside of the right undertray leading edge where the cone hits occurred. As shown in *Figure 122*, the front of the wing insert broke off and needed to be replaced with a steel tab. Also shown in *Figure 122* is an aluminum sheet that was glued over an area on the bottom of the undertray that was punctured by a cone. *Figure 123* shows an area that was punctured on the top. Obviously, the leading edge, which was 2 plies of T800 PW, was a grossly under built, and should have been at least 6 plies.



*Figure 122: Broken undertray wing insert replaced with steel tab*



*Figure 123: Leading edge damage*

Another component that broke was the M4 potted insert in the undertray for the drop link on the right side. It is unknown whether the pull-out occurred because of poor bonding, or if it did indeed exceed the epoxy's strength. Regardless, it was replaced with the flanged M6 flanged potted insert, as shown in *Figure 124*. The flange provides added resistance to pull-out failure.



*Figure 124: M6 flanged potted insert for the drop link*

Lastly, the outer side skirt and front edge of the endplate were quickly worn out from constant exposure to the elements, cone impacts, and from being stepped on. These sections definitely could have used more reinforcement.

## **9. CONCLUSION**

As predicted by lap time simulation, aerodynamic downforce offers huge gains in competitiveness for Formula SAE vehicles. Testing has shown that the best way to produce this desired downforce is with large wings. Wings are less effective (L/D) than undertrays, but Formula SAE vehicles can afford a lot of drag and loss in fuel efficiency at their low speeds. The opposite is true for Formula 1 vehicles, which race at much higher speeds making undertrays have more advantages. Nonetheless, underbody design is still very important for Formula SAE and can easily weaken a vehicle concept if not done correctly. While current testing does not offer too much insight into the exact performance of the undertray documented in this thesis, the inverted airfoil concept has merit and should at the very least, be incorporated into the side-pod design.

## **10. WORKS CITED**

- [1] "2013 Formula SAE Rules," SAE International, 2012.
- [2] S. a. J. S. Wordley, "Aerodynamics for Formula SAE: Initial design and performance prediction," SAE International, 2005.
- [3] K. Jenson, "Aerodynamic Undertray Design for Formula SAE," Oregon State University, Corvallis, OR, 2010.
- [4] S. McBeath, Competition Car Aerodynamics, Sparkford, Yeovil, Somerset, UK: Haynes Publishing, 2006.
- [5] J. Katz, New Directions in Race Car Aerodynamics, Cambridge, MA: Bentley Publishers, 2006.
- [6] S. Wordley and J. Saunders, "Aerodynamics for Formula SAE: A Numerical, Wind Tunnel and On-Track Study," 2005.
- [7] S. McBeath, Competition Car Composites: A Practical Handbook, Sparkford: Haynes Publishing, 2010.
- [8] A. B. Strong, Fundamentals of Composites Manufacturing, Dearborn, MI: Society of Manufacturing Engineers, 2008.
- [9] "Formula Student Combustion Rules 2013," Formula Student Germany, 2012.
- [10] "Formula Student Electric Rules 2013," Formula Student Germany, 2012.
- [11] Toray Carbon Fibers America, Inc., 2008. [Online]. Available: <http://www.toraycfa.com/pdfs/T800HDataSheet.pdf>.
- [12] Hexcel Corporation, 2013. [Online]. Available:

[http://www.hexcel.com/Resources/DataSheets/Honeycomb-Data-Sheets/HRH\\_10\\_us.pdf](http://www.hexcel.com/Resources/DataSheets/Honeycomb-Data-Sheets/HRH_10_us.pdf).

[13] Fiberlay Inc., 2001. [Online]. Available: <http://www.fiberlay.com/upload/techd-360502012-HYSOL%209430%20TDS.pdf>.

[14] Fiberlay Inc., 2001. [Online]. Available: <http://www.scottsales.com/Epoxy-Patch-Kits/HysA9340-EN.pdf>.

[15] Krayden, Inc., 2007. [Online]. Available:  
[http://krayden.com/tds/hunts\\_renshape\\_5008\\_tds.pdf](http://krayden.com/tds/hunts_renshape_5008_tds.pdf).

[16] RenShape Solutions, 2002. [Online]. Available:  
<http://www.freemansupply.com/datasheets/RenPatchRenWeld5008.pdf>.

